PROCEEDINGS A

rspa.royalsocietypublishing.org

Research

Article submitted to journal

Subject Areas:
Structural Engineering

Keywords:
rigid-foldability, generic rigid-foldability, folding, configuration

Author for correspondence:
Zeyuan He
e-mail: zh299@cam.ac.uk

THE ROYAL SOCIETY
PUBLISHING

On Rigid Origami I: Piecewise-planar Paper with Straight-line Creases

Zeyuan He[1], Simon D. Guest[2]

[1,2]Department of Engineering, University of Cambridge, Cambridge CB2 1PZ, United Kingdom

Origami (paper folding) is an effective tool for transforming two-dimensional materials into three-dimensional structures, and has been widely applied to robots, deployable structures, metamaterials, etc. Rigid origami is an important branch of origami where the facets are rigid, focusing on the kinematics of a panel-hinge model. Here we develop a theoretical framework for rigid origami, and show how this framework can be used to connect rigid origami and its cognate areas, such as the rigidity theory, graph theory, linkage folding and computer science. First, we give definitions regarding fundamental aspects of rigid origami, then focus on how to describe the configuration space of a creased paper. The shape and 0-connectedness of the configuration space are analyzed using algebraic, geometric and numeric methods. In the algebraic part we study the tangent space and generic rigid-foldability based on the polynomial nature of constraints for a panel-hinge system. In the geometric part we analyze corresponding spherical linkage folding and discuss the special case when there is no cycle in the interior of a crease pattern. In the numeric part we review methods to trace folding motion and avoid self-intersection. Our results will be instructive for the mathematical and engineering design of origami structures.

1. Introduction

This article develops a general theoretical framework for rigid origami, and shows how rigid origami is linked with other related areas, such as the rigidity theory, graph theory, linkage folding, and computer science.

Origami has been used for many different physical models, as a recent review [1] shows. Sometimes a "rigid" origami model is required where all the deformation is concentrated on the rotation along creases. A rigid origami model is usually considered to be a system of rigid panels that are able to rotate around their common boundaries, which has been applied to many areas across different length scales [2]. These successful applications have inspired us to focus on the fundamental theory of rigid origami. Ultimately, we are considering two problems: first, the forward problem, which is to find useful sufficient and necessary conditions for a creased paper to be rigid-foldable; second, the inverse problem, which is to approximate a target surface by rigid origami.

The paper is organized as follows. In Sections 2 and 3 we will clarify the definitions of relevant concepts, such as what we mean by paper and rigid-foldability. In Sections 4, 5 and 6 we will show three methods that can be applied to study rigid origami. Specifically, an algebraic method (linked to rigidity theory and graph theory), a geometric method (linked to linkage folding), and a numerical method (linked to computer science). Some comments and a brief discussion on some important downstream open problems on rigid origami conclude the paper.

2. Modelling

In this section we start with some basic definitions for *origami*. Although the idea of *folding* can be precisely described by isometry excluding Euclidean motion, the definition of paper needs to be carefully considered: we want our mathematical definition to correspond with the commonly understood properties of a paper in the physical world. A paper should not just be a surface in $\mathbb{R}^3$. At any point, there might be contact of different parts of a paper, although crossing is not allowed. We introduce the idea of a *generalized surface* in Definition 1 that allows multiple layers local to a point, and in Definition 4 exclude all the crossing cases with the help of an *order function* in Definition 3. The definitions we make in this section are based on Sections 11.4 and 11.5 in [3] with appropriate modifications and extensions – for example, we don't require a paper to be orientable, and we allow contact of different parts of a paper.

Definition 1. We first consider a *connected piecewise-C^1 2-manifold M* (possibly with boundary, defined in Sections 12.3 and 15.2, [4]). Here "piecewise-C^1" means that countable piecewise-C^1 curves can be removed from M in such a way that the remainder decomposes into countable C^1 open 2-manifolds, and M is required to be a closed set. Every point on each piece has a well-defined tangent space, and a Euclidean metric is equipped such that the length of a piecewise-C^1 curve connecting two points on M can be measured.

A *generalized surface* $g(M)$ is a subset of $\mathbb{R}^3$, where $g: M \to \mathbb{R}^3$ is a piecewise immersion. A *piecewise immersion* is a continuous and piecewise-C^1 function whose derivative is injective on each piece of M. Hence $g(M)$ is still connected and a closed set. The *distance* of two points $g(p)$ and $g(q)$ on $g(M)$ ($p, q \in M$) is defined as the infimum of the lengths of $g(\gamma)$, where γ is a piecewise-C^1 curve connecting p and q on M.

The definition on a generalized surface is an extension of how we usually define a connected piecewise-C^1 surface in $\mathbb{R}^3$ (Section 12.2, [4]). As stated above, Definition 1 is still not enough to prevent crossing of different parts of a paper, for which we introduce the definition of *crease pattern* and *order function*.

Definition 2. A *crease pattern* G is a simple graph embedding on a generalized surface $g(M)$, that contains the boundary of those pieces. Each edge of G is a C^1 curve on $g(M)$. Note that the boundary of $g(M)$ is also part of the graph G, which is written as $\partial g(M) = g(\partial M) \subset G$. A *crease* is an edge of G without the endpoints, and those endpoints are called *vertices*. A vertex or crease is *inner* if it is not on the boundary $\partial g(M)$, otherwise *outer*; and a piece as *inner* if none of its vertices is on $\partial g(M)$, otherwise *outer*.

To introduce the order of stacking on different parts of a paper, we need the information of normal vector on $g(M)$. Now considering a point $p \in M$ and $g(p) \notin G$, there are two coordinate frames of the tangent space (left-handed and right-handed) of $g(p)$, which have opposite orientation. Therefore the orientability and orientation of $g(M)$ can be defined in the same way as a piecewise-C^1 surface in $\mathbb{R}^3$, which are described in Section 12.3, [4]. The following definition on order function depends on the orientability of $g(M)$.

Definition 3. If $p, q \in M$, $g(p), g(q) \notin G$ and $g(p) = g(q)$, an *order function* λ is defined on p, q that describes the order of stacking of layers locally. If $g(M)$ is orientable, all the tangent spaces have a consistent orientation, then let $\lambda(p, q) = 1$ if p is in the direction pointed to by the normal vector $\boldsymbol{n}_g(q)$ (on the "top" side of q); and $\lambda(p, q) = -1$ if p is in the direction pointed to by $-\boldsymbol{n}_g(q)$ (on the "bottom" side of q). If $g(M)$ is non-orientable, it can always be divided into countable orientable generalized surfaces (called *parts*) that abut along some of their boundaries. The reason is the range of charts together $\{U_i\}$ cover $g(M)$, and $g(M)$ has countable topological bases, hence $\{U_i\}$ has a countable subcover $\{U_j\}$. Each U_j in this subcover can be assigned an orientation, then $g(M)$ can be described as the union of some subsets of $\{U_j\}$ that abut along some of their boundaries. For example, a Möbius band is the union of two orientable surfaces (Section 12.3, [4]) that abut along two components of their boundaries. By assigning a specified orientation of each part, the order of stacking can still be described using the order function, since now each non-crease point is assigned a normal vector, which is consistent inside each part. Each boundary of parts can be allocated to one of its adjacent parts, so there is no difficulty if the contact point is on the boundary of parts. Note that $g(M)$ is still not orientable because the parts altogether will have inconsistent orientation.

Definition 4. A generalized surface S is a *paper* if there exists a crease pattern G, such that S makes the order function λ satisfy the four conditions described in Section 11.4 of [3], which prevent the crossing of paper.

Remark 1. A generalized surface is required to be a closed set since it is physically reasonable for a paper to contain its boundary. A generalized surface is required to be connected since otherwise it is the union of countable connected generalized surfaces (also called its components), and in that case each component is a paper. Definition 4 prevents crossing of different parts of a paper when they contact with each other. The contact of a point with a crease point is allowed, but the conditions for order function can not be satisfied if there is a crossing. A paper does not need to be developable or bounded.

Figure 1 shows some examples of objects which are, and are not, papers.

Definition 5. Here the *folded state* and *folding motion* are defined for a creased paper. A *creased paper* (S, G) is a pair of a paper S and a crease pattern G. A *folded state* of a creased paper (S, G) is a pair (f, λ), where f is an isometry function excluding Euclidean motion that maps (S, G) to another creased paper $(f(S), f(G))$ and preserves the distance; λ is the order function of $(f(S), f(G))$. A folded state is *free* when the domain of the order function is empty. The identity map with its order function (I, λ) is the *trivial* folded state.

A *folding motion* is a family of continuous functions mapping each time $t \in [0, 1]$ to a folded state (f_t, λ_t). The continuity of f_t is defined under the *supremum metric*, $\forall t \in [0, 1]$, $\forall \epsilon > 0$, $\exists \delta > 0$ s.t. if $|t' - t| < \delta$

$$\sup_{p \in S} ||f_{t'}(p) - f_t(p)|| < \epsilon \tag{2.1}$$

If S is orientable, the continuity of λ_t with respect to t is described in Section 11.5 of [3]. If S is not orientable, when its order function is defined, S is divided into orientable parts and each part is assigned an orientation. Then at each non-crease contact point, the continuity of λ_t with respect to t should follow Section 11.5 of [3].

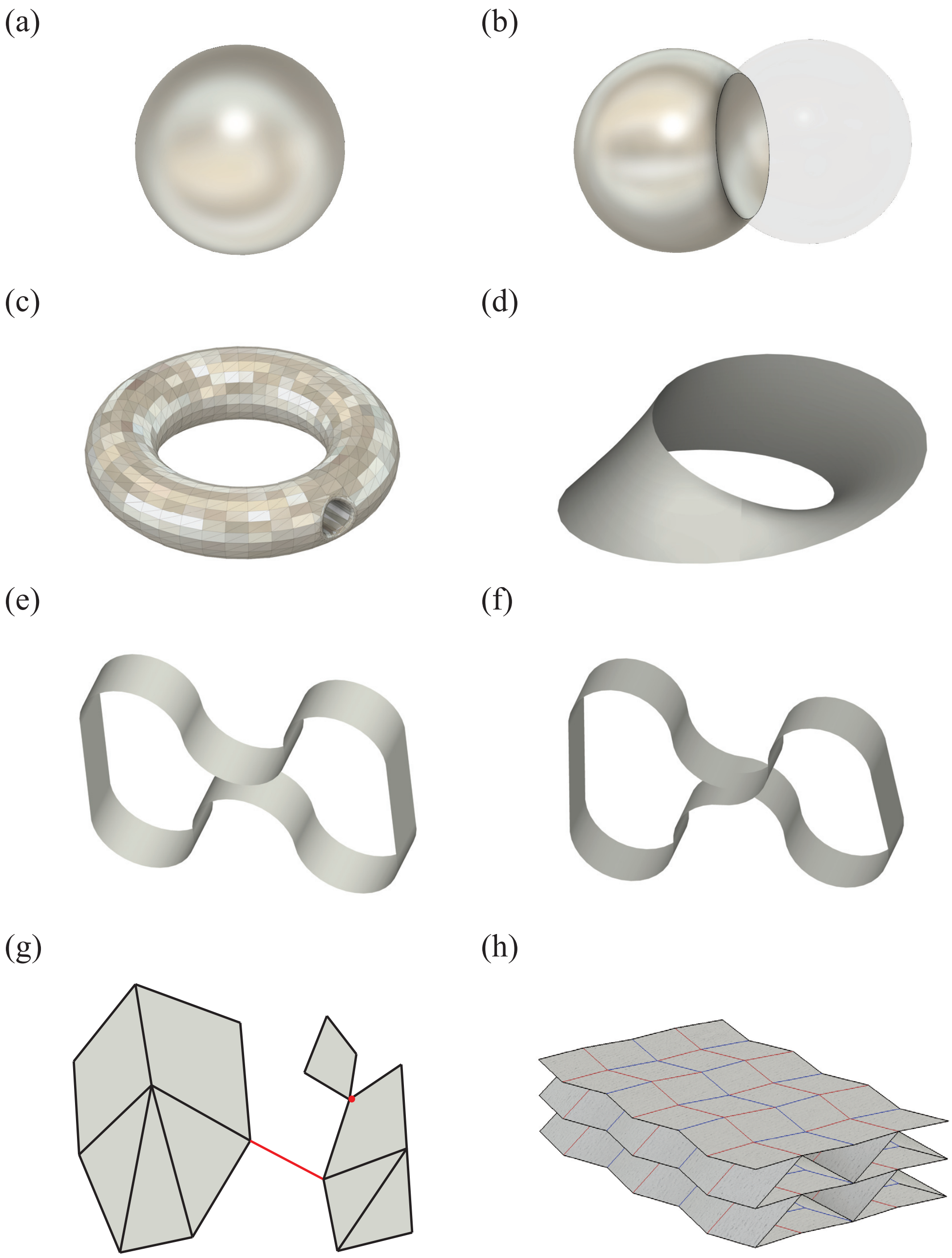

Figure 1. Examples of objects that do, or do not, conform to the definition of "paper" used in this article. (a)–(e) are papers with unusual shapes. (a) is a sphere, which can be regarded as a paper. (b) is a folded state of (a) with a curved crease, generated by the intersection of two identical spheres. (c) is a piecewise-planar paper with two dough-nut holes (Euler Characteristic -2). (d) is a Möbius band, an example of non-orientable surface, which is the union of two orientable surfaces that abut along two components of their boundaries. (e) shows the case where there is contact between different parts of a paper. (f)–(h) are "paper-like" objects that are not papers even though they might be physically "foldable". (f) is similar to (e), but the two layers intersect with each other, hence it does not satisfy the condition on the order function. Part of (g) is 1-dimensional. It can be regarded as a foldable mechanism with a spherical joint and a bar (colored red). (h) is an example of the stacking meta-material, where the contact points are crease points. It is not connected following the requirement of a paper, instead it can be regarded as the union of five papers (plotted by Freeform Origami [5]).

If there is a folding motion between two different folded states (f_1, λ_1) and (f_2, λ_2), (f_1, λ_1) is *foldable* to (f_2, λ_2), and the creased paper is *foldable*. If (f, λ) is not foldable to any other folded state, this folded state is *rigid*.

Remark 2. Mapping a creased paper to another creased paper requires the isometry function f to be a piecewise immersion. When excluding the self-intersected configurations and defining the folding motion of a creased paper, we rely on the technical statements on order function provided in Sections 11.4 and 11.5 of [3].

Based on the definitions above, now we start to discuss rigid origami. The only difference between origami and rigid origami is the restriction of f on each piece.

Definition 6. A *rigidly folded state* is a folded state where the restriction of the isometry function f on each piece is a combination of translation and rotation. A *rigid folding motion* is a folding motion where all the folded states are rigidly folded states.

Remark 3. Reflection is not included in the isometry function of rigid origami restricted to a piece.

From Definition 6, since each piece is under a combination of translation and rotation, we can make appropriate simplification on the creased paper (S, G). First, we can require each inner crease to be a straight-line, otherwise the two pieces adjacent to this inner crease will not have relative rigid folding motion, which is not what we expect in rigid origami. Second, for clarity all pieces are chosen to be planar, but note that there would be no essential difference in the results presented here without this restriction. Therefore,

Definition 7. In rigid origami, our object of study can be limited to a creased paper (P, C) with a *piecewise-planar* paper P and a *straight-line* crease pattern C. Here each planar piece is called a *panel*. The set of all rigidly folded states $\{(f, \lambda)\}_{P,C}$ is called the *rigidly folded state space*.

As an alternative way to move from origami to rigid origami, [6] shows that an isometric map on a creased paper will become piecewise rigid if we require the paper S, crease pattern G and isometry function f to have stronger properties. This result is provided in Appendix (a).

In the following section, we will start to discuss the configuration of a creased paper (P, C) in rigid origami.

3. The Configuration Map of a Creased Paper in Rigid Origami

In order to study the rigid-foldability between possible rigidly folded states of a creased paper, in this section we introduce the configuration map to characterize a rigidly folded state. Before that, some preliminary definitions are needed.

Definition 8. At every vertex, the angles between adjacent creases are *sector angles*, each of which is named α_i. $\boldsymbol{\alpha} = \{\alpha_i\}$ is the set of all sector angles, which are regarded as fixed variables under a given creased paper (P, C), satisfying:

$$\alpha_i \in (0, 2\pi); \text{ except that, for a degree-1 vertex, } \alpha = 2\pi$$

Then we specify an orientation for (P, C) (If P is not orientable, an orientation is assigned to each part of its division as mentioned in Definition 3). At each inner crease, a signed *folding angle* ρ_j is defined by which the two panels adjacent to the inner crease deviate from a plane, specifically, ρ_j is the difference between π and the dihedral angle measured from the specified orientation.

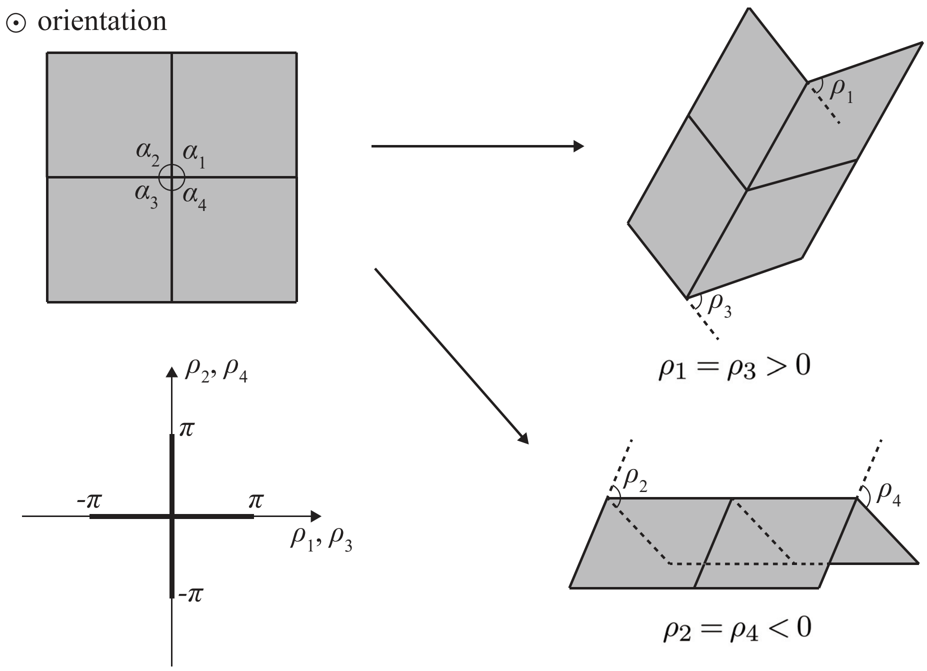

Figure 2. Here we show a simple creased paper with four sector angles $\alpha_1 = \alpha_2 = \alpha_3 = \alpha_4 = \pi/2$, and its two rigidly folded states with $\rho_1 = \rho_3 > 0$, $\rho_2 = \rho_4 = 0$ and $\rho_2 = \rho_4 < 0$, $\rho_1 = \rho_3 = 0$. The folding angles are measured in the specified orientation, which is the "top" side of the paper, facing the readers. The configuration space is a "cross", and the information of stacking is contained in the difference of $\rho_j = \pm\pi$. The configuration map is a bijection from the configuration space to the rigidly folded state space.

$\boldsymbol{\rho} = \{\rho_j\}$ is the set of all folding angles, satisfying:

$$\rho_j \in [-\pi, \pi]$$

The sector and folding angles are illustrated in Figure 2.

We introduce the sector and folding angles in order to find an explicit expression for the isometry function f of a rigidly folded state for any point $p \in P$ and a given $\boldsymbol{\rho}$. The set of folding angles of the trivial rigidly folded state is denoted by $\boldsymbol{\rho}_0$, which is not necessarily $\mathbf{0}$.

From the analysis above, a rigidly folded state (f, λ) corresponds with a set of folding angles $\boldsymbol{\rho}$. However, different (f, λ) can be mapped to the same $\boldsymbol{\rho}$ — an example is shown in Figure 3. The difference in $\rho_j = \pm\pi$ can only represent the information of order function on two panels adjacent to an inner crease. Therefore the order function is still needed when expressing a rigidly folded state with $\boldsymbol{\rho}$.

Proposition 1. Given a creased paper (P, C), a panel P_0 is fixed to exclude Euclidean motion. Set one of the vertices as the origin and one of its creases labelled c_0 as the x-axis. then build the right-hand *global coordinate system* with xy-plane on this panel. For every $p \in P$, $p = [x, y, z]^T$, there is a path from the origin $(0, 0, 0)$ to p. The path intersects with C on some inner creases labelled c_k ($k \in [1, K]$). The folding angle on crease c_k is ρ_k (Figure 4).

A *local coordinate system* can also be built on panel P_k ($k \in [1, K]$), whose origin O_k is on one endpoint of c_k, x-axis is on c_k and z-axis is normal to the panel. p is in the closure of P_K. The direction of all z-axes of the global and local coordinate systems are consistent with the orientation of the paper and hence consistent with the definition of the sign of folding angles. The direction of the x-axis is specified on c_k so that the rotation from panel P_{k-1} to P_k is a rotation of the define

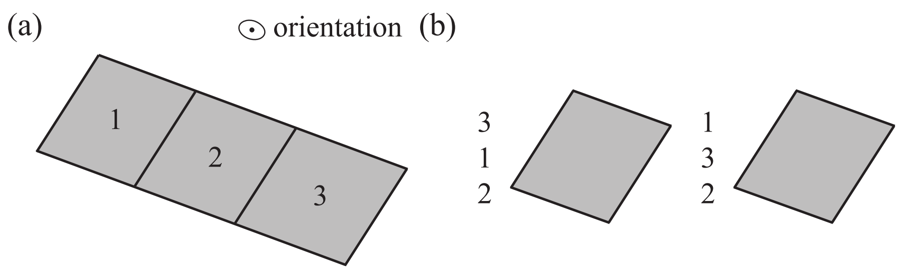

Figure 3. (a) is a creased paper with three identical squares. Here the orientation is chosen to be the "top" side of the paper, facing the readers. (b) shows two different rigidly folded states of (a) with the same folding angle $\{-\pi, -\pi\}$. The numbers are stacking sequences of the panels. The order functions of these two rigidly folded states are $\lambda(1,3)=1$, $\lambda(3,1)=-1$ and $\lambda(1,3)=-1$, $\lambda(3,1)=1$.

folding angle ρ_k about that axis. The angle between the x-axes of local coordinate systems on creases c_{k-1} and c_k as β_k. β_k is a linear function of the sector angles $\boldsymbol{\alpha}$.

Now the coordinate of p in the local coordinate system can be written as $f^K(p) = [f_x^K(p), f_y^K(p), f_z^K(p)]^T$. When using homogeneous matrices to represent the transformation from local to global coordinate system along the path, the result is:

$$\begin{bmatrix} f(p) \\ \\ 1 \end{bmatrix} = \begin{bmatrix} f_x(p) \\ f_y(p) \\ f_z(p) \\ 1 \end{bmatrix} = T_K(\boldsymbol{\rho}) \begin{bmatrix} f_x^K(p) \\ f_y^K(p) \\ f_z^K(p) \\ 1 \end{bmatrix} \tag{3.1}$$

where,

$$T_K(\boldsymbol{\rho}) = \prod_1^K \begin{bmatrix} \cos\beta_k & -\sin\beta_k & 0 & a_k \\ \sin\beta_k & \cos\beta_k & 0 & b_k \\ 0 & 0 & 1 & 0 \\ 0 & 0 & 0 & 1 \end{bmatrix} \begin{bmatrix} 1 & 0 & 0 & 0 \\ 0 & \cos\rho_k & -\sin\rho_k & 0 \\ 0 & \sin\rho_k & \cos\rho_k & 0 \\ 0 & 0 & 0 & 1 \end{bmatrix} \tag{3.2}$$

$[a_k, b_k, 0]^T$ $(k \in [1, K])$ is the position of O_k in the local coordinate system for panel P_{k-1}. The product T is formed by post-multiplication.

Let $\boldsymbol{\rho} = \boldsymbol{\rho}_0$:

$$\begin{bmatrix} x \\ y \\ z \\ 1 \end{bmatrix} = T_K(\boldsymbol{\rho}_0) \begin{bmatrix} x^K \\ y^K \\ z^K \\ 1 \end{bmatrix} \tag{3.3}$$

where $[x^K, y^K, z^K]$ is the coordinate of p in the local coordinate system on panel K. As panel P_K moves rigidly, we have

$$\begin{bmatrix} f_x^K(p) \\ f_y^K(p) \\ f_z^K(p) \\ 1 \end{bmatrix} = \begin{bmatrix} x^K \\ y^K \\ z^K \\ 1 \end{bmatrix} \tag{3.4}$$

Thus,

$$\begin{bmatrix} f_x(p) \\ f_y(p) \\ f_z(p) \\ 1 \end{bmatrix} = T_K(\boldsymbol{\rho}) T_K^{-1}(\boldsymbol{\rho}_0) \begin{bmatrix} x \\ y \\ z \\ 1 \end{bmatrix} \tag{3.5}$$

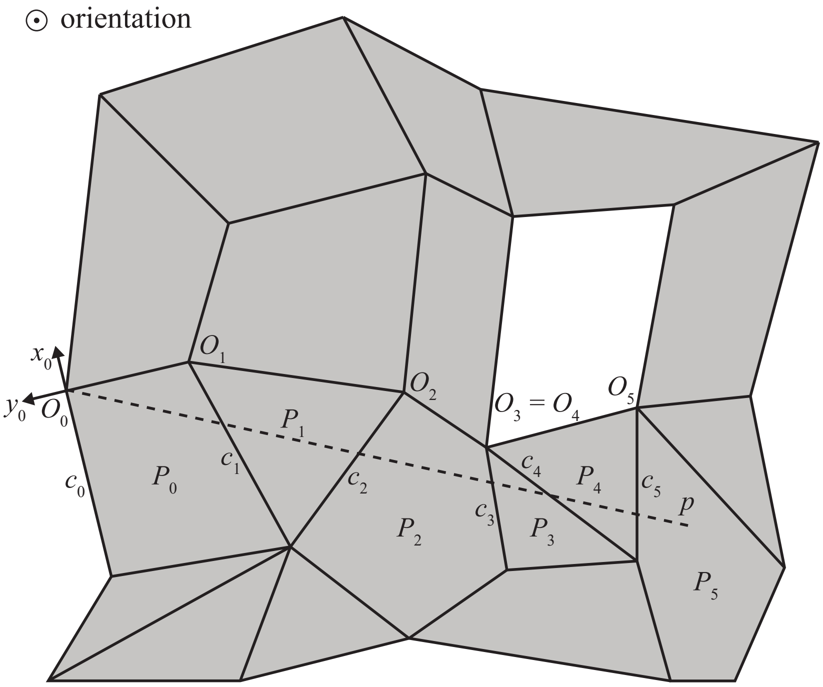

Figure 4. A creased paper with two boundary components (Euler characteristic 0). Here the orientation is chosen to be the "top" side of the paper, facing the readers. The point p, intermediate inner creases c_k, panels P_k and origins O_k ($k \in [0, 5]$) are shown respectively. The position of p can be described by a series of rotation and translation starting from O_0.

Remark 4. In Definition 3, the order function is defined on the non-crease contact points, and in rigid origami pairs of points on stacked panels will have the same order function. Note that simply describing the order of stacking for panels is not sufficient for a well-defined order. An example is the Möbius band triangle, where ordering of the three panels a, b, c are $a > b > c > a$ ($>$ means on the top side of).

Definition 9. Given a creased paper (P, C), the *configuration map* is defined as $F : \{(\boldsymbol{\rho}, \lambda)\}_{P,C} \to \{(f, \lambda)\}_{P,C}$, where $\{\boldsymbol{\rho}\}_{P,C}$ is the set of folding angles of all possible rigidly folded states of (P, C), and $\{\lambda\}_{P,C}$ is the collection of order function for each $\boldsymbol{\rho}$. The collection of this pair $\{(\boldsymbol{\rho}, \lambda)\}_{P,C}$ is called the *configuration space*. An example of the configuration map and configuration space is provided in Figure 2. Now F naturally becomes a bijection. The order function λ can be a multivalued function of $\boldsymbol{\rho}$ in the configuration space, and when using $\boldsymbol{\rho}$ to describe the configuration, λ does not need to include the stacking of adjacent panels since this information is included in the difference of $\rho_j = \pm\pi$.

Before further discussion we want to explain the limit of $\boldsymbol{\rho}$, f and λ in the configuration space. A series of $\{\boldsymbol{\rho}_n\} \to \boldsymbol{\rho}$ is naturally defined; $\{f_n\} \to f$ means the supreme metric $\sup |f_n(p) - f(p)| \to 0$; $\{\lambda_n\} \to \lambda$ requires $\{\lambda_n\}$ to satisfy the continuity condition mentioned in Section 11.5 of [3]. These conditions for $\{\lambda_n\}$ are to guarantee there is no crossing in the approach of a series of rigidly folded states.

Proposition 2. The configuration map F has the following properties:

(1) F is *scale-independent*. That means, if inflating P to P' by a factor c $(g>0)$, for any $p'=cp$, $f(p')=cf(p)$; if an order function is defined on p,q, and $p'=cp$, $q'=cq$ then $\lambda(p',q')=\lambda(p,q)$.
(2) We extend f to be the function of $\boldsymbol{\rho}$, $\boldsymbol{\rho}_0$ and p, then

$$f(-\boldsymbol{\rho},-\boldsymbol{\rho}_0,\begin{bmatrix} x \\ y \\ -z \end{bmatrix})=\begin{bmatrix} 1 & 0 & 0 \\ 0 & 1 & 0 \\ 0 & 0 & -1 \end{bmatrix} f(\boldsymbol{\rho},\boldsymbol{\rho}_0,\begin{bmatrix} x \\ y \\ z \end{bmatrix})$$

Therefore the positions of $f(-\boldsymbol{\rho},-\boldsymbol{\rho}_0)$ and $f(\boldsymbol{\rho},\boldsymbol{\rho}_0)$ are symmetric to P_0, $\{\boldsymbol{\rho}\}_{P,C}$ is symmetric to $\mathbf{0}$, and $\lambda(-\boldsymbol{\rho})=-\lambda(\boldsymbol{\rho})$.
(3) If F is defined in a neighborhood of a point in $\{(\boldsymbol{\rho},\lambda)\}_{P,C}$, or F^{-1} is defined in a neighborhood of a point in $\{(f,\lambda)\}_{P,C}$, F is a homeomorphism.
(4) $\{\boldsymbol{\rho}\}_{P,C}$ is discrete or compact.

Proof. Statement (1): Inflating P means to keep all the sector angles and inflate the lengths of all the creases by c, so for any $p'=cp$, direct calculation gives $f(p')=cf(p)$. Also, inflating does not change the order function.

Statement (2): This expression is equivalent to:

$$T_K(-\boldsymbol{\rho})T_K^{-1}(-\boldsymbol{\rho}_0)\begin{bmatrix} x \\ y \\ -z \\ 1 \end{bmatrix}=\begin{bmatrix} 1 & 0 & 0 & 0 \\ 0 & 1 & 0 & 0 \\ 0 & 0 & -1 & 0 \\ 0 & 0 & 0 & 1 \end{bmatrix} T_K(\boldsymbol{\rho})T_K^{-1}(\boldsymbol{\rho}_0)\begin{bmatrix} x \\ y \\ z \\ 1 \end{bmatrix} \tag{3.6}$$

which can be proved by induction and direct symbolic calculation. When changing all the folding angles $\boldsymbol{\rho}$ to $-\boldsymbol{\rho}$ and calculate λ from the same orientation, the order of panels is reversed, so $\lambda(-\boldsymbol{\rho})=-\lambda(\boldsymbol{\rho})$.

Statement (3): In the neighborhood of $(\boldsymbol{\rho},\lambda)$ that F is defined, for any series of $(\boldsymbol{\rho}_n,\lambda_n)\to(\boldsymbol{\rho},\lambda)$, we need to prove $(f_n,\lambda_n)\to(f,\lambda)$. This is guaranteed because f is smooth with respect to $\boldsymbol{\rho}$. We also need to prove that for any series of $(f_n,\lambda_n)\to(f,\lambda)$ we have $(\boldsymbol{\rho}_n,\lambda_n)\to(\boldsymbol{\rho},\lambda)$. This is because if $\sup|f_n(p)-f(p)|\to 0$, $T_{nK}(\boldsymbol{\rho})-T_K(\boldsymbol{\rho})\to 0$, then $\boldsymbol{\rho}_n\to\boldsymbol{\rho}$ with the information in order function. The case for F^{-1} defined in a neighborhood of a point in $\{(f,\lambda)\}_{P,C}$ is similar.

Statement (4): If $\{\boldsymbol{\rho}\}_{P,C}$ is not discrete, the rigidly folded state space $\{(f,\lambda)\}_{P,C}$ is closed in the sense the limit of f and λ are defined, since the properties of an isometry function f and order function λ are preserved under limitation. From statement (3), $\{\boldsymbol{\rho}\}_{P,C}$ is closed. Because $\{\boldsymbol{\rho}\}_{P,C}$ is also bounded, it is compact. □

Since it is more convenient to study the rigid-foldability in the configuration space rather than in the rigidly folded state space, we provide the next conclusion.

Theorem 1. Given a creased paper (P,C), (f_1,λ_1) is rigid-foldable to (f_2,λ_2) if and only if $(\boldsymbol{\rho}_1,\lambda_1)$ is 0-connected to $(\boldsymbol{\rho}_2,\lambda_2)$ in the configuration space $\{(\boldsymbol{\rho},\lambda)\}_{P,C}$.

Proof. The following proof is an extension of "The combination of continuous functions is continuous."

Sufficiency: If $(\boldsymbol{\rho}_1,\lambda_1)$ and $(\boldsymbol{\rho}_2,\lambda_2)$ are 0-connected in $\{(\boldsymbol{\rho},\lambda)\}_{P,C}$, this path is parametrized by $L:t\in[0,1]\to\{(\boldsymbol{\rho},\lambda)\}_{P,C}$. From statement (3) in Proposition 2, on this path L, the configuration map $F:\{(\boldsymbol{\rho},\lambda)\}_{P,C}\to\{(f,\lambda)\}_{P,C}$ is continuous. It can be directly verified that the composite map $F\circ L:t\in[0,1]\to\{(f,\lambda)\}_{P,C}$ is also continuous. Therefore (f_1,λ_1) is rigid-foldable to (f_2,λ_2).

Necessity: (f_1,λ_1) is rigid-foldable to (f_2,λ_2) means there exists a path in this function space $L':t\in[0,1]\to\{(f,\lambda)\}_{P,C}$. Every point on this path corresponds with a point in the configuration space $\{(\boldsymbol{\rho},\lambda)\}_{P,C}$, and from statement (3) in Proposition 2, the inverse of configuration map $F^{-1}:\{(f,\lambda)\}_{P,C}\to\{(\boldsymbol{\rho},\lambda)\}_{P,C}$ is continuous on L'. Similarly we can verify that the composite map $F^{-1} \circ L' : t \in [0,1] \to \{(\boldsymbol{\rho}, \lambda)\}_{P,C}$ is also continuous. Therefore $(\boldsymbol{\rho}_1, \lambda_1)$ and $(\boldsymbol{\rho}_2, \lambda_2)$ are 0-connected. □

Definition 10. If the configuration space is a collection of discrete points, it is called 0-*dimensional*. If the configuration space is $(\mathbf{0}, \emptyset)$ or a collection of two points $(\boldsymbol{\rho}, \lambda)$ and $(-\boldsymbol{\rho}, -\lambda)$, it is named *trivial*, and this creased paper is *globally rigid*.

From Theorem 1, the existence of non-trivial rigidly folded states and rigid-foldability are the shape and 0-connectedness of the configuration space $\{(\boldsymbol{\rho}, \lambda)\}_{P,C}$, which are not easily characterized. We will mainly present three methods to study the configuration space: algebraic, geometric and numeric methods. Usually we focus on $\{\boldsymbol{\rho}\}_{P,C}$ and then check λ when there are multiple λ for a particular $\boldsymbol{\rho}$. For convenience from now on we use $(\boldsymbol{\rho}, \lambda)$ to represent a rigidly folded state.

4. Algebraic Analysis of the Configuration Space

The algebraic method analyzes the possible position of panels around vertices (equation (4.1)) and holes (equation (4.2)) symbolically, then remove the solutions that induce self-intersection of panels. Before further discussion some definitions are needed.

Definition 11. Given a creased paper (P, C), $W_{P,C}$ is the solution space of the *consistency constraints* given in equations (4.1) and (4.2), where every $\rho_j \in [-\pi, \pi]$.

(1) At every inner degree-n vertex: (Figure 5(a))

$$T_n(\boldsymbol{\rho}) = \prod_1^n \begin{bmatrix} \cos\alpha_j & -\sin\alpha_j & 0 \\ \sin\alpha_j & \cos\alpha_j & 0 \\ 0 & 0 & 1 \end{bmatrix} \begin{bmatrix} 1 & 0 & 0 \\ 0 & \cos\rho_j & -\sin\rho_j \\ 0 & \sin\rho_j & \cos\rho_j \end{bmatrix} = I \tag{4.1}$$

where α_j is between c_{j-1} and c_j $(j \in [2,n])$, α_1 is between c_n and c_1. Equation (4.1) can be derived by following Proposition 1 and choosing the path to be the one shown in Figure 5(a). T is formed by post-multiplication. Only three of the nine equations are independent, which are in different columns and rows.

(2) For a hole with n inner creases (Figure 5(b)), called a *degree-n* hole: (If the Euler Characteristic is 2 or 1, there is no such constraint)

$$T_n(\boldsymbol{\rho}) = \prod_1^n \begin{bmatrix} \cos\beta_j & -\sin\beta_j & 0 & a_j \\ \sin\beta_j & \cos\beta_j & 0 & b_j \\ 0 & 0 & 1 & 0 \\ 0 & 0 & 0 & 1 \end{bmatrix} \begin{bmatrix} 1 & 0 & 0 & 0 \\ 0 & \cos\rho_j & -\sin\rho_j & 0 \\ 0 & \sin\rho_j & \cos\rho_j & 0 \\ 0 & 0 & 0 & 1 \end{bmatrix} = I \tag{4.2}$$

where β_j is between c_{j-1} and c_j $(j \in [2,n])$, β_1 is between c_n and c_1. $[a_j, b_j, 0]$ $(j \in [1,n])$ is the position of O_j in the local coordinate system for panel P_{j-1}. Equation (4.2) can be derived by following Proposition 1 and choosing the path to be the one shown in Figure 5(b). T is formed by post-multiplication. Only six of the sixteen equations are independent. Three of them are in the top left 3×3 rotation matrix, the other three are the elements from row 1 to row 3 in column 4, which are automatically satisfied if the inner creases are concurrent.

The consistency constraints may not include every folding angle, so $\widetilde{W}_{P,C}$ is defined as the *extension* of the solution space $W_{P,C}$ to include the folding angles not mentioned in $W_{P,C}$, also with range $[-\pi, \pi]$. $N_{P,C}$ is the collection of all the solutions that do not satisfy the conditions for order function λ, i.e. panels self-intersect, which are called the *boundary constraints* because they are unilateral constraints that only contribute to the boundary of $\{\boldsymbol{\rho}\}_{P,C}$. Some examples have been mentioned in [7].

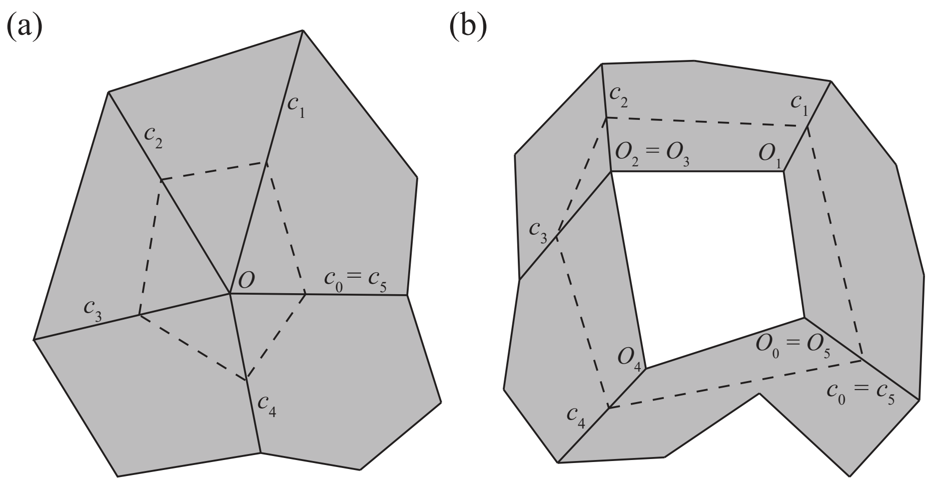

Figure 5. (a) is a degree-5 single-vertex creased paper. (b) is a degree-5 single-hole creased paper. For each creased paper, a path is shown to illustrate the consistency constraints in Definition 11. We label intermediate inner creases c_j and origins O_j ($j \in [0, 5]$). Note that (a) has one boundary component and (b) has two boundary components. We don't need to consider the consistency constraint around the outer boundary because it is naturally satisfied (Definition 11).

Remark 5. Although the lengths of creases may not be involved in the consistency constraints, they are important in the boundary constraints. In a large creased paper, a folding angle will appear in the consistency constraints once or twice, generating a coupled system.

Theorem 2. [7,8]

$$\{\boldsymbol{\rho}\}_{P,C} = \widetilde{W}_{P,C} \backslash N_{P,C} \tag{4.3}$$

Corollary 2.1. Some properties of $W_{P,C}$ and $N_{P,C}$.

(1) $W_{P,C}$ is symmetric to $\mathbf{0}$, so $N_{P,C}$ is symmetric to $\mathbf{0}$.
(2) $W_{P,C}$ is discrete or compact, so $N_{P,C}$ is open and bounded if not discrete.

Proof. Statement (1) can be proved by comparing the expressions of $T_n(\boldsymbol{\rho}) + T_n(-\boldsymbol{\rho})$ and $T_n(\boldsymbol{\rho}) - T_n(-\boldsymbol{\rho})$. With induction and direct symbolic calculation, if $T_n(\boldsymbol{\rho}) = 0$, $T_n(-\boldsymbol{\rho}) = 0$. Because $\{\boldsymbol{\rho}\}_{P,C}$ is also symmetric to $\mathbf{0}$, $N_{P,C}$ is symmetric to $\mathbf{0}$. Statement (2) is satisfied because if $W_{P,C}$ is not a discrete set, any limit point of $W_{P,C}$ is also a solution, which means $W_{P,C}$ is closed, also, $W_{P,C}$ is bounded. □

From Definition 11, the consistency constraints are derived from the consistency of panels around an inner vertex or a hole, therefore we define:

Definition 12. Given a creased paper (P, C), for each inner vertex v, the restriction of (P, C) on all panels incident to v forms a *single-vertex creased paper*, and v is called the *centre vertex* (Figure 5(a)). Similarly, consider a hole with boundary h, whose incident inner creases are not concurrent. The restriction of (P, C) on all panels incident to h forms a *single-hole creased paper* (Figure 5(b)). If the inner creases incident to a hole are concurrent, it is still regarded as a single-vertex creased paper, whose centre vertex is the intersection of its inner creases. A single-vertex or single-hole creased paper is called a *single creased paper*. The number of folding angles is the *degree* of a single creased paper.

Corollary 2.2. $\widetilde{W}_{P,C}$ is the intersection of extensions of the solution spaces of all single creased papers.

Corollary 2.2 clarifies the link between global and local rigid-foldability, and explains why local rigid-foldability cannot guarantee global rigid-foldability, since even the intersection of 0-connected spaces is not necessarily 0-connected.

Next we want to apply results in the classic rigidity theory based on the consistency constraints. Here elements $\{(3,2),(1,3),(2,1)\}$ are chosen as independent constraints from each equation (4.1) and from the top left 3×3 of equation (4.2). This is because considering the first-order derivative of T [9]:

$$\frac{\partial T}{\partial \rho_j} = \begin{bmatrix} 0 & -z_j & y_j \\ z_j & 0 & -x_j \\ -y_j & x_j & 0 \end{bmatrix} \tag{4.4}$$

where $[x_j, y_j, z_j]$ is the direction vector of inner crease c_j for ρ_j in the coordinate system built on ρ_n, pointing outside the centre vertex or hole. Therefore only choosing non-diagonal elements from each equation (4.1) or top left 3×3 of equation (4.2) could result in a valid first-order derivative, which corresponds with the direction of "speed" in kinematics. The collection of independent consistency constraints is written as $\boldsymbol{A}(\boldsymbol{\rho}) = \boldsymbol{0}$, whose solution space is larger than $W_{P,C}$. If verifying the solution of $\boldsymbol{A}(\boldsymbol{\rho}) = \boldsymbol{0}$ with equations (4.1) and (4.2), the result could be some rotation matrices containing 0 and ± 1 other than I, but they can be easily removed.

Further, by using the *normalized folding angles* $\boldsymbol{t}: t_j = \tan\frac{\rho_j}{2}$ ($t_j \in [-\infty, \infty]$), the independent consistency constraints can be written as a system of polynomial equations $\boldsymbol{A}(\boldsymbol{t}) = \boldsymbol{0}$ with:

$$\cos\rho_j = \frac{1-t_j^2}{1+t_j^2}, \quad \sin\rho_j = \frac{2t_j}{1+t_j^2} \tag{4.5}$$

For convenience, in this section we will mainly use the above representation $\boldsymbol{A}(\boldsymbol{t}) = \boldsymbol{0}$ for further analysis. The degree for each folding angle in each equation of $\boldsymbol{A}(\boldsymbol{t}) = \boldsymbol{0}$ is at most 2.

(a) Equivalent Definitions on Rigid-foldability

Here we will follow the idea that is commonly understood for bar-joint frameworks, and give several equivalent definitions on rigid-foldability, which also holds if expressed by the folding angles $\boldsymbol{\rho}$.

Definition 13. An *analytic path* $\gamma: [s_1, s_2] \ni s \to \{(\boldsymbol{t}, \lambda)\}_{P,C}$ that joins $(\boldsymbol{t}_1, \lambda_1)$ and $(\boldsymbol{t}_2, \lambda_2)$ can be expressed as:

$$t_i(s) = \sum_{n=0}^{\infty} a_{in}(s-s_1)^n \tag{4.6}$$

where t_i are the components of γ and a_{in} are the coefficients for the power series of t_i.

Theorem 3. Given a creased paper (P, C), the three following definitions on rigid-foldability are equivalent.

(1) (Analytic) Given a rigidly folded state ($\boldsymbol{t}$, λ), if there exists another rigidly folded state ($\boldsymbol{t}'$, λ'), where $\boldsymbol{t}'$ is connected to $\boldsymbol{t}$ in the folding angle space $\{\boldsymbol{t}\}_{P,C}$ by an analytic path, and λ' is 0-connected to λ, then ($\boldsymbol{t}$, λ) is rigid-foldable to ($\boldsymbol{t}'$, λ').

(2) (Continuous) Given a rigidly folded state ($\boldsymbol{t}$, λ), if there exists another rigidly folded state ($\boldsymbol{t}'$, λ') which is 0-connected to ($\boldsymbol{t}$, λ) in the configuration space, then ($\boldsymbol{t}$, λ) is rigid-foldable to ($\boldsymbol{t}'$, λ').

(3) (Topological) Given a rigidly folded state $(\boldsymbol{t}, \lambda)$, $\forall \epsilon > 0$, if there exists another rigidly folded state $(\boldsymbol{t}_\epsilon, \lambda_\epsilon)$, s.t. $0 < |\boldsymbol{t}_\epsilon - \boldsymbol{t}| < \epsilon$, and all $\{\lambda_\epsilon\}$ satisfy the continuity condition mentioned in Section 11.5 of [3], then $(\boldsymbol{t}, \lambda)$ is rigid-foldable.

Proof. (1) $\rightarrow$ (2) and (2) $\rightarrow$ (3) are natural. Next we prove (3) $\rightarrow$ (1). If from (3), $(\boldsymbol{t}, \lambda)$ is rigid-foldable, then $\boldsymbol{t}$ is a limit point of the solution of $\boldsymbol{A}(\boldsymbol{t}) = \boldsymbol{0}$. From the curve selection lemma (Section 3, [10]), there exists a real analytic curve γ starting from $\boldsymbol{t}$ and ending at another point $\boldsymbol{t}'$. The continuity of order function is naturally satisfied since the path in (1) is selected from (3). $\square$

Corollary 3.1. If two points in the configuration space are only connected by a single path, this curve is analytic. For example, the configuration space of a rigid-foldable degree-4 single-vertex creased paper or a rigid-foldable quadrilateral creased paper [11] is analytic.

(b) Analysis from the Tangent Space

Given a creased paper (P, C) and a point $(\boldsymbol{t}, \lambda)$ in the configuration space, it is traditional in kinematics to consider the possible "infinitesimal" motion and determine the direction of "speed" in the configuration space. An "infinitesimal flex", or a *first-order flex* $\mathrm{d}\boldsymbol{t}$, is a vector in the tangent space of $\boldsymbol{t}$ satisfying $\mathrm{J}\boldsymbol{A} \cdot \mathrm{d}\boldsymbol{t} = \boldsymbol{0}$, where $\mathrm{J}\boldsymbol{A} = \mathrm{d}\boldsymbol{A}/\mathrm{d}\boldsymbol{t}$ is the Jabocian. Here $\mathrm{J}\boldsymbol{A}$ is a formal derivative since a point in the configuration space might be discrete. If (P, C) has i inner vertices, j inner creases and h holes, the number of equations is $3i + 6h$, while the number of variables is j, hence the size of $\mathrm{J}\boldsymbol{A}$ is $(3i + 6h) \times j$. If $\mathrm{rank}(\mathrm{J}\boldsymbol{A}) = \min(3i + 6h, j)$, i.e. reaches its maximum, this rigidly folded state $(\boldsymbol{t}, \lambda)$ is *regular*, otherwise it is *special*. If denoting the degree of freedom by $\deg(\boldsymbol{t}) = j - \mathrm{rank}(\mathrm{J}\boldsymbol{A})$, $\{\boldsymbol{t}\}_{P,C}$ is locally a $\deg(\boldsymbol{t})$ dimensional smooth manifold. It also has a $\deg(\boldsymbol{t})$ dimensional tangent space. If $\deg(\boldsymbol{t}) = 0$, i.e. the only first-order flex is $\boldsymbol{0}$, this rigidly folded state $(\boldsymbol{t}, \lambda)$ is *first-order rigid*, otherwise *first-order rigid-foldable*. For a regular point, the counting of degree of freedom is provided in [12].

Theorem 4. (1) If $(\boldsymbol{t}, \lambda)$ is first-order rigid, it is rigid. Equivalently, if $(\boldsymbol{t}, \lambda)$ is rigid-foldable, it is first-order rigid-foldable.
(2) If $(\boldsymbol{t}, \lambda)$ is regular and rigid, it is first-order rigid. Equivalently, if $(\boldsymbol{t}, \lambda)$ is regular and first-order rigid-foldable, it is rigid-foldable.

Proof. Statement (1): If for a given point $\boldsymbol{t}$, $\boldsymbol{A}(\boldsymbol{t}) = \boldsymbol{0}$ and $\deg(\boldsymbol{t}) = 0$, from the Implicit Function Theorem (Section 8.5, [4]), $\boldsymbol{A}^{-1}(\boldsymbol{0})$ is a 0-dimensional manifold in some neighborhood of $\boldsymbol{t}$, hence $(\boldsymbol{t}, \lambda)$ is rigid.

Statement (2): If $\boldsymbol{t}$ is a regular point, from the Implicit Function Theorem, the dimension of $\boldsymbol{A}^{-1}(\boldsymbol{0})$ in a neighborhood of $\boldsymbol{t}$ equals to $\deg(\boldsymbol{t})$. Therefore if $(\boldsymbol{t}, \lambda)$ is regular, $(\boldsymbol{t}, \lambda)$ is rigid if and only if $(\boldsymbol{t}, \lambda)$ is first-order rigid. $\square$

Remark 6. For a smooth creased paper (the origami case), the foldability and rigidity can be similarly defined in the topological or continuous sense. However, here the first-order rigidity does not imply rigidity, while analytical first-order rigidity implies analytical rigidity, which means that these definitions on foldability are not equivalent. For details please refer to Chapter 12, [13].

Note that unlike a bar-joint framework, projective and affine transformation does not preserve the first-order rigidity or first-order rigid-foldability.

(c) Generic Rigid-foldability and Equivalent Panel-hinge Framework

When studying the rigid-foldability of creased papers, we find that some of them with a crease pattern isomorphic to a particular graph might be (almost) always rigid, or might be (almost) always rigid-foldable. This is the combinatorial property of a crease pattern, which is called the generic rigidity (or rigid-foldability). Here we will discuss the theory of generic rigidity, starting from a discussion on first-order rigidity. This is parallel to the work on the generic rigidity of bar-joint frameworks [14].

Definition 14. Given a graph H, $(P,C)_H$ is defined as a creased paper with a crease pattern isomorphic to H, which is also called a *realization* of H. $\{(P,C)\}_H$ is the collection of such creased papers, and $\{\boldsymbol{t}\}_H$ is the collection of normalized folding angles of such creased papers.

Theorem 5. (1) Either (a) the set $X=\{\boldsymbol{t}|(P,C)_H$ is first-order rigid$\}$ is an open dense subset in $\{\boldsymbol{t}\}_H$, and (almost) all realizations of H are first-order rigid; or (b) $X=\emptyset$ and all realizations of H are first-order rigid-foldable.

(2) Either (a) the set $Y=\{\boldsymbol{t}|(P,C)_H$ is rigid$\}$ contains an open dense subset in $\{\boldsymbol{t}\}_H$, and (almost) all realizations of H are rigid; or (b) $Y^c=\{\boldsymbol{t}|(P,C)_H$ is rigid-foldable$\}$ contains an open dense subset in $\{\boldsymbol{t}\}_H$, and (almost) all realizations of H are rigid-foldable.

Proof. Statement (1): Assume that there is a first-order rigid realization $(\boldsymbol{t},\lambda)$ for a given graph H, then $\deg(\boldsymbol{t})=0$, or equivalently, some sub-matrices of $\mathrm{J}\boldsymbol{A}$ have non-zero determinants. This is a system of polynomial constraints over $\boldsymbol{t}$. If such a system of polynomials is non-zero at $\boldsymbol{t}$, it is non-zero in an open dense subset of $\{\boldsymbol{t}\}_H$ (Section 3 of [15]).

Statement (2): Assume that there is a first-order rigid realization $(\boldsymbol{t},\lambda)$ for a given graph H, from Theorem 4, $Y\supset X$, so the first part holds. Then assume there is no first-order rigid realization, Y^c contains all regular realizations of H, which are defined as $R=\{\boldsymbol{t}|$some sub-matrices of $\mathrm{J}\boldsymbol{A}$ have non-zero determinants$\}$ (a *regular realization* is where the Jacobian has maximum rank). This is also a system of polynomial constraints over $\boldsymbol{t}$. If such a system of polynomials is non-zero at $\boldsymbol{t}$, it is non-zero in an open dense subset of $\{\boldsymbol{t}\}_H$. □

Definition 15. From Theorem 5, several equivalent definitions are provided on the *generic rigidity* of H. If H is not generically rigid, it is *generically rigid-foldable*.

(1) H is generically rigid if X is dense in $\{\boldsymbol{t}\}_H$, or equivalently, (almost) all realizations of H are first-order rigid.
(2) H is generically rigid if there is a first-order rigid realization.
(3) H is generically rigid if there is a first-order rigid regular realization.

A *generic realization* of H is a rigid realization if H is generically rigid, or is a rigid-foldable realization if H is generically rigid-foldable.

Remark 7. For a bar-joint framework, "generic realization" usually means the coordinates of its vertices do not satisfy a system of polynomial equations with rational coefficients, which is a strong sufficient condition for genericity. However, in rigid origami we use folding angles to describe the position of a creased paper, and a similar statement has not been found. How to exactly determine whether a realization is generic is still unclear in both classic rigidity theory and rigid origami. Sometimes estimating the generic rigidity from the number of constraints, for example saying "H is generically rigid if $3i+6h\geq j$", will fail for a similar reason to the “double banana” model in bar-joint frameworks [16]. Often, finding a non-generic rigid-foldable realization for a generically rigid crease pattern is an important topic, where tools such as symmetry might be useful. For instance, the Miura-ori [17] is a non-generic realization of a quadrilateral crease pattern, that is generically rigid.

A creased paper (P,C) can be regarded as a panel-hinge framework in rigidity theory, if each panel is considered as a rigid body and the vertices on each panel are constrained in a plane. Here is a conclusion connecting the property of H and the generic rigidity of H.

Definition 16. Given a graph H, its *dual graph* H^* is a graph that has a vertex for each face of H, and has an edge whenever two faces of H are separated from each other by an edge. A *multigraph* kH ($k \in \mathbb{Z}$) is defined as replacing each edge of H by k parallel edges. A *spanning tree* of H is a subset of H, which has all the vertices covered with minimum possible number of edges.

Theorem 6. H is generically rigid if and only if $5H^*$ contains 6 edge-disjoint spanning trees [18].

Global rigidity (Definition 10) is also an important concept in classic rigidity theory, but there is no complete result on the generic global rigidity for a panel-hinge framework. It would be very appealing to develop a parallel theory that connects the property of H and the generic global rigidity of H.

Remark 8. Modelling rigid origami by a corresponding bar-joint framework with position-based description is often used for numerical simulation, which can be generated by replacing each panel with a complete bar graph. This process can be described using graph product for a periodic crease pattern [19]. A corresponding bar-joint framework also allows the discussion for engineering based non-rigid origami, for example, there might be elastic deformation along the bars [20]. However, even assuming all bars are rigid, this modelling only preserves the finite motion, while the first-order flex will be completely different without additional constraints. Therefore when studying the kinematics of rigid origami, it is probably better to use the folding angle description.

(d) High order Rigid-foldability

We want the concept of high order rigid-foldability to be a generalization of the first-order rigid-foldability. It is natural to consider the Taylor expansion of $\boldsymbol{A}(\boldsymbol{t}) = \boldsymbol{0}$ near a point in the configuration space. The n-th order flex is an ordered pair $(\boldsymbol{\rho}', \boldsymbol{\rho}'', ...\boldsymbol{\rho}^{(n)})$ that satisfies the equation given by the first n terms of Taylor expansion. If the solution space of the n-th order flex is $(\boldsymbol{0}, \boldsymbol{0}, ...\boldsymbol{0})$, the creased paper is *$n$-th order rigid*, otherwise *n-th order rigid-foldable*. The problem is, as stated before, the degree for each folding angle in $\boldsymbol{A}(\boldsymbol{t}) = \boldsymbol{0}$ is at most 2. Given a creased paper, if the degree of its single creased papers is at most m, the $(2m+1)$-th derivative of $\boldsymbol{A}(\boldsymbol{t}) = \boldsymbol{0}$ will vanish. Hence only up to $2m$-th order flex is sensible if the high-order rigid-foldability is defined in this way, which also means at most $2m$-th order rigid-foldability implies rigid-foldability.

When calculating the derivatives, it was found that the folding angle expression $\boldsymbol{A}(\boldsymbol{\rho}) = \boldsymbol{0}$ leads to a simpler form. [21] gives explicit constraints for the first-order and second-order flex.

(e) Duality and Isomorphism of the Tangent Space, Figure Method

From the constraints on the first-order and second-order flex, [21] also gives the following conclusions on a developable creased paper, which includes the discussion on reciprocal figure of the crease pattern. We will introduce related definitions first.

Definition 17. Given a planar crease pattern C, the *reciprocal figure* R is a mapping (with potential self-intersection) from a dual graph C^* (Definition 16) of C on to a plane with the following properties:

(1) The edge c^* in R mapped from a crease c in C is a line segment perpendicular to c.
(2) The face loop is defined for each face v^* in R corresponding to vertex v in C as the sequence of dual edges corresponding to the edges in counterclockwise order around v.
(3) Each edge c^* of the reciprocal diagram has assigned a sign σ_i, such that along any face loop of v^*, the direction of the edge c^* is 90° clockwise or counterclockwise rotation of

the vector along the original crease c from corresponding vertex v if the sign is plus or minus, respectively.

A *zero-area* reciprocal diagram of C is a reciprocal diagram of C where the signed area of each face in the counterclockwise orientation is zero. Example figures are shown in [21].

Theorem 7. Main results in [21].

(1) A developable creased paper (P, C) is first-order rigid-foldable if and only if there exists a non-trivial (not a point) reciprocal figure of C.
(2) A developable creased paper (P, C) is second-order rigid-foldable if and only if there exists a non-trivial zero-area reciprocal figure of C.
(3) For a developable single-vertex creased paper, the second-order rigid-foldability is equivalent to rigid-foldability.
(4) For a developable and flat-foldable quadrilateral creased paper [11], the second-order rigid-foldability is equivalent to rigid-foldability.

Remark 9. Statements (3) and (4) imply a very interesting topic, which is to find the minimum order m leading to the equivalence of mth-order rigid-foldability to rigid-foldability for some special creased papers. We believe that there must be some deeper reason to justify the equivalence of high-order rigid-foldability and rigid-foldability for a certain type of creased paper, possibly from real algebraic geometry, which will be discussed in a future article.

Along with the analyses above, there are also some isomorphism on the tangent space $T_{\boldsymbol{\rho}}$ for a developable creased paper. From the constraints on the first-order flex, $T_{\boldsymbol{\rho}}$ is isomorphic to the space of the magnitude of admissible axial forces, when regarding the inner creases as rigid bars, and the holes as rigid panels. It means that $\mathrm{d}\boldsymbol{\rho} \in T_{\boldsymbol{\rho}}$ if and only if the above model is in equilibrium when seeing $\mathrm{d}\boldsymbol{\rho}$ as the magnitude of corresponding axial forces [9].

Proposition 3. The planar state of a developable creased paper is first-order rigid-foldable if the degree of each inner vertex is no less than 4.

Proof. We start from assuming that there is no hole in this developable creased paper (Euler Characteristic 1), which has i inner vertices and j inner creases. From the isomorphism mentioned above, at the planar state $\deg(\mathbf{0}) = j - 2i$. If the degree of each inner vertex is 4 and the creased paper is unbounded, $j = 2i$. However, consider the effect of boundary, each inner vertex share more inner creases, so $j > 2i$, and if there are some vertices whose degree is greater than 4, j will be even greater, therefore $\deg(\mathbf{0}) = j - 2i > 0$. For a developable creased paper with holes, it can be generated by cutting from a developable creased paper without hole, hence its planar state is still first-order rigid-foldable. $\square$

[22] gives another way to describe the constraints on the first-order flex by the existence of dual graph. Assuming a point $\boldsymbol{\rho}$ is differentiable with respect to a parameter t in $\{\boldsymbol{\rho}\}_{P,C}$, then for every K,

$$\dot{\rho_K}\overrightarrow{c_K} = \overrightarrow{\omega_K} - \overrightarrow{\omega_{K-1}} \tag{4.7}$$

$\overrightarrow{c_K}$ is the direction vector of crease c_K where the folding angle is ρ_K, and ω_K is the angular velocity of panel K in the global coordinate system. From Proposition 1:

$$\overrightarrow{\omega_K}(\boldsymbol{\rho})_\times = \dot{T}_K(\boldsymbol{\rho})T_K^T(\boldsymbol{\rho}) \tag{4.8}$$

where:

$$\overrightarrow{\omega_K}(\boldsymbol{\rho})_\times = \begin{bmatrix} 0 & -\omega_z & \omega_y \\ \omega_z & 0 & -\omega_x \\ -\omega_y & \omega_x & 0 \end{bmatrix}$$

$\omega_x, \omega_y, \omega_z$ are the coordinates of $\overrightarrow{\omega_K}(\boldsymbol{\rho})$, and

$$T_K(\boldsymbol{\rho}) = \prod_1^K \begin{bmatrix} \cos\beta_k & -\sin\beta_k & 0 \\ \sin\beta_k & \cos\beta_k & 0 \\ 0 & 0 & 1 \end{bmatrix} \begin{bmatrix} 1 & 0 & 0 \\ 0 & \cos\rho_k & -\sin\rho_k \\ 0 & \sin\rho_k & \cos\rho_k \end{bmatrix}$$

By associating each panel with the instantaneous rotation axis, we get a dual graph C^* of C, which is formed by joining corresponding ends of the instantaneous rotation axes. $\dot{\boldsymbol{\rho}}$ is admissible if and only if C^* is parallel to C.

(f) When the Paper is a Polyhedron

If the paper is a polyhedron, many conclusions from other related topics can be filled into the framework of rigid origami. One classic topic is unfolding a given polyhedron with possible cuts along the edges, and the main problem of it is to avoid self-intersection, which is discussed in Section 6(b). Another topic is to consider the possible rigid folding motion of a polyhedron without cutting. Based on the well-known Cauchy's Theorem, a strictly convex polyhedron is rigid, while a non-convex polyhedron might be rigid-foldable. Robert Connelly gave an example of non-convex rigid-foldable polyhedron [23]. The Bellows Conjecture, saying that the volume of a rigid-foldable polyhedron is invariant under rigid folding motion, was proved and became a typical feature of such rigid-foldable polyhedra [24]. Although studying the isometry of a polyhedron is a historical problem, the research concerning the rigid folding motion between possible isometries is relatively new and there are many open problems.

5. Geometric Analysis of the Configuration Space

As well as the algebraic analysis above, we can also consider a geometrical perspective. The consistency and boundary constraints of the configuration space are the geometric and physical compatibility of the rigid panels.

(a) Connection with Spherical Linkage Folding, Spherical Duality

Spherical linkage folding has proved useful in modelling a single-vertex creased paper. If putting the centre vertex in the centre of a sufficiently small sphere, all the sector angles will correspond to a closed series of great spherical arcs (consistency constraints) that only intersect at the endpoints of all the arcs (boundary constraints), and every folding angle is the supplement of an interior angle of this spherical polygon. Possible rigid folding motion of a single-vertex creased paper can also be descibed from triangulating this spherical linkage. some basic analyses for a degree 1, 2 or 3 single creased paper are provided in Appendix (b).

We then consider the rigid-foldability of a degree-n single-vertex creased paper. In planar linkage folding, the *Carpenter's rule problem* is to ask whether a simple planar polygon can be moved continuously to where all its vertices are in convex position, the edge lengths are preserved and there is no self-intersection along the way [25]. It is foreseeable that the rigid-foldability of a single-vertex creased paper is closely linked with the spherical version of the Carpenter's rule problem.

Proposition 4. Some conclusions about the folding angle space of a degree-n single-vertex creased paper $\{\boldsymbol{\rho}\}_v$ from spherical linkage folding.

(1) If a pair of inner creases is collinear, $\sum \alpha_l \geq 2\pi$. The corresponding folding angles are denoted by ρ_i, ρ_j, then $\{\boldsymbol{\rho}\}_v$ has a two dimensional subspace $\rho_i = \rho_j$.
(2) If a pair of inner creases is collinear, and $\sum \alpha_l = 2\pi$, the corresponding folding angles are denoted by ρ_i, ρ_j, then $\{\boldsymbol{\rho}\}_v$ has a two dimensional subspace $\rho_i = \rho_j$, other $\rho_k = 0$. All these subspaces only intersect at $\mathbf{0}$.

(3) If $\sum \alpha_l \in (0, 2\pi)$, then every $\alpha_l \in (0, \pi)$, and there is no pair of collinear inner creases (antipodal points). $\{\boldsymbol{\rho}\}_v$ is $\{\boldsymbol{\rho}_0, -\boldsymbol{\rho}_0\}$ or the union of two disjoint 0-connected subspaces, which are symmetric to $\mathbf{0}$ [26]. Note that even if $n \geq 4$, the configuration space can be two isolated points, such as $\alpha_1 = \alpha_2 + \alpha_3 + \alpha_4$.
(4) If $\sum \alpha_l = 2\pi$ and every $\alpha_l \in (0, \pi)$, $\{\boldsymbol{\rho}\}_v$ is $\{\mathbf{0}\}$ or the union of two 0-connected subspaces [26], which are symmetric to $\mathbf{0}$ and only intersect at $\mathbf{0}$. If and only if the degree of centre vertex $n \geq 4$ and the interior of crease pattern is not a cross, $\{\boldsymbol{\rho}\}_v$ has other non-trivial 0-connected subspaces different from (2), where every folding angle can be non-zero [27].
(5) Otherwise, from the constraints of a closed spherical linkage, $\sum \alpha_l \in (2\pi, (2n-2)\pi)$. Generically, by arbitrarily given $n-3$ folding angles we can obtain a spherical triangle, and the rest 3 folding angles can be calculated, hence there is no difficulty in simulating a general degree-n vertex.

The point of view from spherical linkage folding is also beneficial when dealing with a multi-vertex system. [28] presented two integrated 1-DOF (single degree of freedom) planar-spherical mechanisms inspired by rigid origami, which also lead to new design of 1-DOF rigid-foldable creased papers. Further, for a general creased paper, it is possible to model it on a sphere with the *Gauss map*. Translating the startpoint of the normal vectors of all panels to the centre of a unit sphere, and connecting the corresponding endpoints on this sphere if they share an inner crease. This operation forms a spherical dual of a creased paper: each panel is mapped to a point, and each inner crease (or each folding angle) is mapped to a linkage. The spherical duality would be a potential tool for analyzing a large creased paper.

(b) When the Interior of Crease Pattern is a Forest

Definition 18. In graph theory, a *forest* is a disjoint union of trees. A *tree* is an undirected graph in which any two vertices are connected by exactly one path.

As stated in the introduction, the forward problem in rigid origami can now be characterized as finding the conditions on sector angles for a creased paper to be rigid-foldable. It is a relatively complex problem because the rigid-foldability of a creased paper cannot be represented by the rigid-foldability of its single creased papers. However, if considering the case where a creased paper has no inner panel, this relatively simple structure may generate rigid-foldability.

Theorem 8. If a creased paper (P, C) satisfies:

(1) The interior of C is a forest.
(2) The restriction of a rigidly folded state $(\boldsymbol{\rho}, \lambda)$ on each single creased paper is rigid-foldable.

then this rigidly folded state $(\boldsymbol{\rho}, \lambda)$ is generically rigid-foldable. Especially, if $\boldsymbol{\rho} = \mathbf{0}$, the configuration $(\boldsymbol{\rho}, \lambda) = (\mathbf{0}, \emptyset)$ is rigid-foldable (Figure 6).

Proof. Since the interior of C is a forest, adjacent single creased papers only share one inner crease. Start from an arbitrary single creased paper, called P^1. Because $(\boldsymbol{\rho}^1, \lambda)$ is not an isolated point (here "isolated" means not 0-connected to any other points), there is a path between a point $(\overline{\boldsymbol{\rho}}^1, \lambda)$ and $(\boldsymbol{\rho}^1, \lambda)$. Consider an adjacent creased paper P^2 with a common folding angle ρ_c. We can write $\rho_c \in [a_1, b_1]$ on the path in $\{(\boldsymbol{\rho}, \lambda)\}^1$, similarly, $\rho_c \in [a_2, b_2]$ on the path in $\{(\boldsymbol{\rho}, \lambda)\}^2$. Let $\rho_c \in [a_1, b_1] \cap [a_2, b_2]$, which is not empty because $\boldsymbol{\rho}$ exists. If $[a_1, b_1] \cap [a_2, b_2]$ is a closed interval, the two paths in $\{(\boldsymbol{\rho}, \lambda)\}^1$ and $\{(\boldsymbol{\rho}, \lambda)\}^2$ can be re-parametrized, then the direct product of them is a path in $\{(\boldsymbol{\rho}, \lambda)\}_{1 \cup 2}$, and now the restriction of this rigidly folded state on $P^1 \cup P^2$ is rigid-foldable. Otherwise, if $[a_1, b_1] \cap [a_2, b_2]$ is just a point, the path may not exist. The case where the

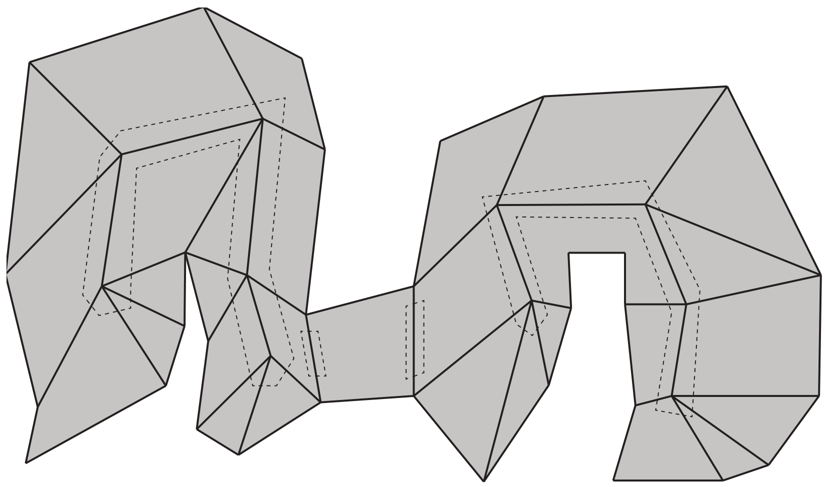

Figure 6. We show a rigid-foldable creased paper with the interior of crease pattern being a forest. Here each tree is denoted by dashed lines.

restriction of $(\boldsymbol{\rho}, \lambda)$ on $\{(\boldsymbol{\rho}, \lambda)\}_{1\cup 2}$ is an isolated point is called non-generic. An example of this non-generic case is shown in Figure 7.

Now consider the special case when $\boldsymbol{\rho} = \mathbf{0}$. This is different to the general case because the range of all folding angles are symmetric to 0. Because $(\mathbf{0}^1, \emptyset)$ is not an isolated point, there must be a path between a point $(\overline{\boldsymbol{\rho}}^1, \lambda)$ and $(\mathbf{0}, \emptyset)$, and from the symmetry there must be a path between $(\mathbf{0}, \emptyset)$ and $(-\overline{\boldsymbol{\rho}}^1, \lambda)$ in $\{(\boldsymbol{\rho}, \lambda)\}^1$. Name its adjacent creased paper P^2 and the common folding angle ρ_c. $\rho_c \in [-a_1, a_1]$ $(a_1 \geq 0)$ on the path in $\{(\boldsymbol{\rho}, \lambda)\}^1$, similarly, $\rho_c \in [-a_2, a_2]$ $(a_2 \geq 0)$ on the path in $\{(\boldsymbol{\rho}, \lambda)\}^2$. Let $\rho_c \in [-\min(a_1, a_2), \min(a_1, a_2)]$, we can always parametrize all the folding angles on $P^1 \cup P^2$ to a continuous path by ρ_c. If a_1 or $a_2 = 0$, the direct product of the two paths in $\{(\boldsymbol{\rho}, \lambda)\}^1$ and $\{(\boldsymbol{\rho}, \lambda)\}^2$ is a new path in the intersection of $\{(\boldsymbol{\rho}, \lambda)\}^1$ and $\{(\boldsymbol{\rho}, \lambda)\}^2$.

Further, the above analysis for each single creased paper can be repeated. Since the number of single creased papers is countable, we can obtain a path between $(\boldsymbol{\rho}, \lambda)$ and another point $(\overline{\boldsymbol{\rho}}, \lambda)$ in the intersection of configuration spaces of all single creased papers if each time we can add a single creased paper in the generic case. If λ is continuous on this path, $(\boldsymbol{\rho}, \lambda)$ is rigid-foldable to $(\overline{\boldsymbol{\rho}}, \lambda)$ along this path. Otherwise, it may be possible to choose a subset of this path to avoid self-intersection of different single creased papers and make λ continuous (so-called generic case). Besides, for $(\mathbf{0}, \emptyset)$, by choosing $\boldsymbol{\rho}'$ on this path sufficiently close to $\boldsymbol{\rho}$, the self-intersection of different single creased papers can be avoided and λ will have no definition, so $(\mathbf{0}, \emptyset)$ is rigid-foldable to $(\boldsymbol{\rho}', \emptyset)$ and $(-\boldsymbol{\rho}', \emptyset)$. □

Remark 10. Theorem 8 is not necessary, even when the interior of C is a forest. If for some single creased papers, the restriction of $(\boldsymbol{\rho}, \lambda)$ is an isolated point, it cannot have relative rigid folding motions, but (P, C) can still be rigid-foldable. If there is a cycle in the interior of C, the path in the intersection of the configuration spaces of all single creased papers may not be successfully generated with the above one-by-one process, and generically $(\boldsymbol{\rho}, \lambda)$ is not rigid-foldable.

Although the general rigid-foldability problem is hard, with Theorem 8, we can analyze some simple creased papers, for instance, quadrilateral creased papers, which will be discussed in a subsequent article.

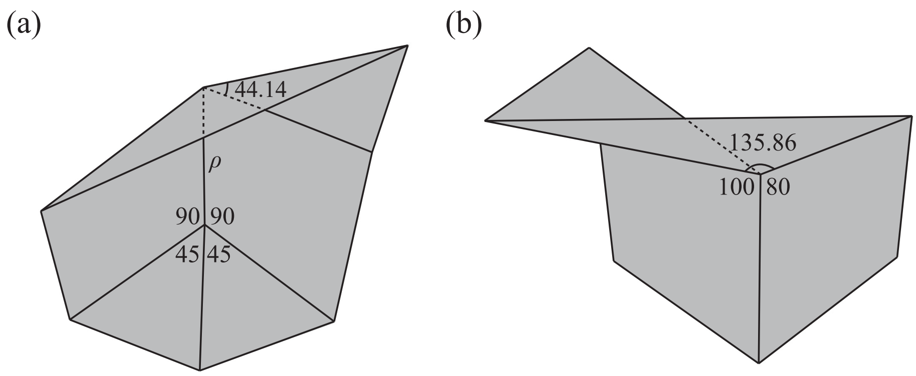

Figure 7. This figure shows a non-generic case mentioned in the proof of Theorem 8. (a) and (b) are the front and rear perspective views of a creased paper, where two single-vertex creased papers share two panels. The sector angles are shown in degrees. This rigidly folded state is not rigid-foldable because the common folding angle ρ cannot exceed $\pi/2$ in the top single-vertex creased paper, and cannot be below $\pi/2$ in the bottom single-vertex creased paper, although both of the single-vertex creased papers are rigid-foldable.

6. Numeric analysis of the Configuration Space

This section gives a brief overview of the numeric analysis on rigid origami. Although this paper concentrates on the algebraic and geometric methods, numerical analysis can be an efficient tool for tracing the rigid folding motion and avoiding self-intersection. We also briefly mention the analysis on complexity of certain problems in rigid origami to give a more complete perspective.

(a) Tracing the Rigid Folding Motion

Given a creased paper (P, C), there are at least two rigidly folded states $(\boldsymbol{t}_0, \lambda(\boldsymbol{t}_0))$ and $(-\boldsymbol{t}_0, -\lambda(\boldsymbol{t}_0))$. A possible way to know its configuration space is to solve the equation $\boldsymbol{A}(\boldsymbol{t}) = \boldsymbol{0}$ introduced in Section 4 numerically, and remove the solutions in $N_{P,C}$. Unfortunately this only works for some small systems, since the total degree of $\boldsymbol{A}(\boldsymbol{t}) = \boldsymbol{0}$ increases dramatically for larger systems. Another way is starting from a point in the configuration space and tracing a possible rigid folding motion based on the integration of first-order flex. An example is given in [29], using the Euler method and correcting errors at each step.

(b) Self-intersection of Panels

In rigid origami, the study on boundary constraints (self-intersection of panels) requires different techniques than those used for the study of consistency constraints. A straightforward question is, how to design a rigid folding motion without self-intersection if a given creased paper is rigid-foldable. The prime source of relevent results comes from the study of unfolding a polyhedron to a planar polygon without overlapping (also called the *net*), which has been extensively studied [30]. However, the result of how to design a rigid folding motion without self-intersection when unfolding a polyhedron is still developing, as introduced below.

It is natural to consider applying a collision detection algorithm to solve the problem of avoiding self-intersection. [31] proposed an algorithm called *Lazy PRM*, which minimizes the number of collision checks performed during robot motion planning and hence minimizes the running time of the planner. Then [32] provided an algorithm under the Lazy PRM framework for cutting and unfolding a polyhedron continuously to one of its nets without self-intersection. This algorithm also works for a "tessellated polyhedron", where each face of a polyhedron is triangulated densely. However, it is still a challenge to unfold a complicated non-convex polyhedron in general if the net is not *linearly foldable* ("linearly foldable" means there exists a straight-line linearly interpolating the planar state to the fully folded state without self-intersection). Further, [33] showed that for a given polyhedron, the way of cutting can be optimized to generate a net that is linearly foldable, *uniformly foldable* ("uniformly foldable" means the speed of each folding angle are the same), and much faster in motion planning than an arbitrary net. Nevertheless, for some complicated non-convex polyhedra such a net may not exist.

There are also some other algorithms for some special creased papers. [34] showed that it is possible to unfold a "nested band" continuously to place all faces of the band into a plane without self-intersection by cutting along exactly one edge. However, the technique used here is extended from one dimensional folding, which seems hard to be applied universally. [35] proved that the source unfolding [30] of any convex polyhedron can be continuously unfolded without self-intersection. Further, any convex polyhedron can be continuously unfolded without self-intersection after a linear number of cuts. Although here the rigid folding motion can be constructed in polynomial time, the source unfolding itself is difficult to compute.

(c) Complexity

Computer-aided design is common for origami, and there have been many results on the complexity of algorithm in origami problems. Here we are more interested in analyses related to rigid origami. [36] showed that it is NP-hard to determine whether a given creased paper can be folded flat (using all the inner creases). [3] showed that it only takes linear time to determine whether a single-vertex creased paper can be folded flat (using all the inner creases). A recent result [37] showed that it is weakly NP-hard to determine whether a degree-4 creased paper (all the inner vertices are degree-4) can be folded flat (using all the inner creases), and it is strongly NP-hard to determine whether a given creased paper is rigid-foldable (using optimal inner creases). The analysis of complexity gives insight for the case where we want to approximate a target surface by sub-dividing the crease pattern.

7. Discussion

(a) Flat-foldability of Rigid Origami

The definition of rigid origami in this paper allows the discussion on flat-foldability. A creased paper is *flat-foldable* if and only if it has a different flat rigidly folded state, where all the folding angles are $\pm\pi$. Note that flat-foldability does not require a rigid folding motion. There have been many conclusions, some of which are collected in [3], including the flat-foldability of a strip (1-dimensional origami), a single-vertex creased paper, and the map folding. [11] provides the sufficient and necessary condition for the flat-foldability of a large quadrilateral creased paper.

(b) Mountain-valley Assignment

Definition 19. A *mountain-valley assignment* of a creased paper is a discrete map of every inner crease μ: $\{c_j\} \to \{M, V\}$. If the folding angle of an inner crease is negative, this inner crease is called a *mountain crease* (M), while if it is positive, this inner crease is called a *valley crease* (V).

This concept is widely used. However, counting possible mountain-valley assignments is known to be a difficult problem. The mountain-valley assignment is of interest here because for a developable creased paper different mountain-valley assignment can classify different branches of rigid folding motion. For a flat-foldable single-vertex creased paper, current progress is given in [38]. For a rigid-foldable single-vertex creased paper [27] or Miura-ori [39], the idea of *minimal forcing set* helps to analyze the mountain-valley assignment. Given a rigid-foldable creased paper and a mountain-valley assignment μ, The *forcing set* is a subset of inner creases such that the only possible mountain-valley assignment for this creased paper that agrees with μ on the forcing set is

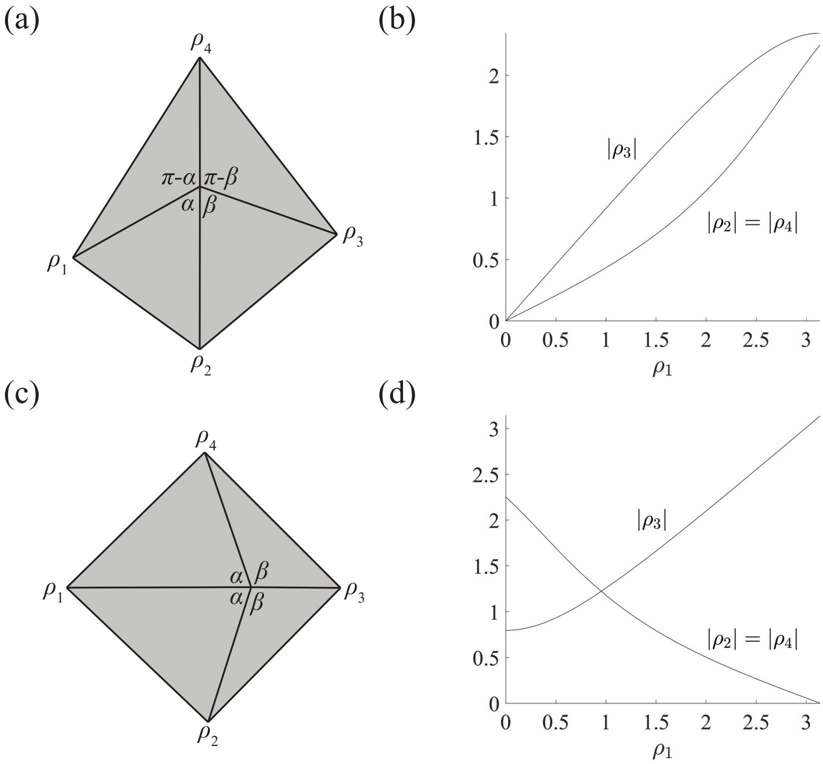

Figure 8. Examples for monotonous rigid-foldability. (a) is a developable degree-4 single-vertex creased paper, while (c) is non-developable (top view). In both examples $\alpha = 60°$, $\beta = 70°$. As ρ_1 increases from 0 to π, the changes of absolute value for ρ_2, ρ_3, ρ_4 in (a) and (c) are shown in (b) and (d) respectively. Here (a) is monotonously rigid-foldable, corresponding to an expansive motion. (c) is not monotonously rigid-foldable.

μ itself. If a forcing set has minimal size among all the forcing sets, it is called the *minimal forcing set*. The theory for the mountain-valley assignment of a large creased paper is still developing, although given a specific example there are some techniques (at least, enumeration) to deal with it. An approach is linking this problem to graph coloring, [40] counts the number of mountain-valley assignments for local flat-foldability of a Miura-ori, while how to identify those guarantee global flat-foldability (which are the real number of branches) requires some unknown techniques. For a non-developable creased paper, the mountain-valley assignment cannot be used to classify its rigid folding motions. Generically, a rigid-foldable creased paper with more symmetry will have more branches of rigid folding motion.

(c) Monotonous Rigid-foldability

If for two rigidly folded states $(\boldsymbol{\rho}_1, \lambda_1)$ and $(\boldsymbol{\rho}_2, \lambda_2)$ of a creased paper (P, C), there exists a path $L: t \in [0,1] \to \{(\boldsymbol{\rho}, \lambda)\}_{P,C}$, s.t. $L(0) = \boldsymbol{\rho}_1$, $L(1) = \boldsymbol{\rho}_2$, and the absolute value for components $|\rho_j(t)|$ (strictly) all increase or all decrease, we say $(\boldsymbol{\rho}_1, \lambda_1)$ is (*strictly*) *monotonously rigid-foldable* to $(\boldsymbol{\rho}_2, \lambda_2)$. This concept is an extension of the *expansive rigid folding motion* mentioned in [26]. In Figure 8, we show a monotonously rigid-foldable single vertex in (a) and (b); and a not monotonously rigid-foldable single vertex in (c) and (d). Monotonous rigid-foldability is a stronger property than 0-connectedness in the configuration space. A better understanding of monotonous rigid-foldability might prove to be useful, for instance in selecting an expansive rigid folding motion that can avoid local self-intersection.

(d) Variation for a Given Crease Pattern

If the interior of a crease pattern is fixed, the shape of panels and the outer creases are not related to the consistency constraints of a rigidly folded state, thus we can reshape the panels and the outer creases to obtain a different creased paper, which will not essentially change the configuration space.

(e) Kirigami

Kirigami can be defined as cutting along countable continuous curves on a creased paper. If a cut curve is closed, a region whose boundary is this cut curve will be removed, otherwise a cut curve will be split into two boundary components. How kirigami will affect the rigid-foldability has not been fully studied, although clearly kirigami will not decrease the rigid-foldability of a creased paper. We intend to discuss this in a future article.

8. Conclusion

This article puts forward a theoretical framework for rigid origami, and demonstrates how this framework can be used to connect rigid origami and results from related areas, such as the rigidity theory, graph theory, linkage folding and computer science. In particular we clarify necessary definitions for rigid origami, and show that the key problem is to describe the shape and 0-connectedness of the configuration space. Further, by using the normalized folding angle expression, we are able to describe the generic and n-th order rigid-foldability from the polynomial nature of a rigid origami system.

Appendix

(a) An Alternative Way to Move from Origami to Rigid Origami

Here a result in [6] is presented: an isometric map on a creased paper will become piecewise rigid if the paper S, crease pattern G and isometry function f are required to have stronger properties. Following Definitions 1–5, we add the conditions below,

(1) S is piecewise-C^2.
(2) If a point on a crease c is C^0 or $c \subset \partial S$, c is a line segment.
(3) A point on a crease or piece of (S, G) is locally isometric to a disk or a half-disk. A vertex of (S, G) is not necessarily locally isometric to a disk or a half-disk.
(4) f is an isometry function such that $f(S)$ is piecewise-C^2.

Then if all "folding angles" are non-trivial,

(1) Each piece is planar.
(2) The restriction of f on each piece is a combination of translation and rotation (reflection is not necessary).

(b) The Configuration Space of a Degree-1, 2 and 3 Single Creased Paper

Here we consider the folding angle space of a degree-n single-vertex and single-hole creased paper, called $\{\boldsymbol{\rho}\}_v^n$ and $\{\boldsymbol{\rho}\}_h^n$, from the solution space W_v^n and W_h^n. When $n \le 3$, the order function has no definition.

(1) W_v^1: $\rho_1 = 0$, when $\alpha_1 = 2\pi$. $\{\boldsymbol{\rho}\}_v^1 = W_v^1$, which is the same for W_h^1 and $\{\boldsymbol{\rho}\}_h^1$ with $\beta_1 = 2\pi$ and $a_1 = b_1 = 0$.

The folding angle on an inner crease incident to a degree-1 vertex is always 0, which means this single creased paper can be regarded as a panel. On the other hand, if a single-hole creased paper has only one inner crease, this single creased paper as well as the hole should always keep planar, which means they can be merged to a panel. Therefore in a large creased paper we only need to consider at least degree-2 single creased papers.

(2) W_h^2 is either (for W_v^2, set $\alpha_1 = \beta_1$, $\alpha_2 = \beta_2$, $a_1 = b_1 = a_2 = b_2 = 0$)

(a) $\rho_1 = \rho_2$, when $\beta_1 = \beta_2 = \pi$, $a_1 = a_2$, $b_1 = b_2 = 0$.
(b) $\rho_1 = \rho_2 = 0$, when $\beta_1 + \beta_2 = 2\pi$, and

$$\begin{aligned} a_1 + a_2 \cos\beta_1 - b_2 \sin\beta_1 = 0 \\ b_1 + a_2 \sin\beta_1 + b_2 \cos\beta_1 = 0 \end{aligned} \tag{A 1}$$

(c) $\rho_1 = \pm\pi$, $\rho_2 = \pm\pi$, when $\beta_1 = \beta_2$, and

$$\begin{aligned} a_1 + a_2 \cos\beta_1 + b_2 \sin\beta_1 = 0 \\ b_1 + a_2 \sin\beta_1 - b_2 \cos\beta_1 = 0 \end{aligned} \tag{A 2}$$

$\{\boldsymbol{\rho}\}_h^2$ is either (for $\{\boldsymbol{\rho}\}_v^2$, set $\alpha_1 = \beta_1$, $\alpha_2 = \beta_2$, $a_1 = b_1 = a_2 = b_2 = 0$)

(a) $\rho_1 = \rho_2$, when $\beta_1 = \beta_2 = \pi$, $a_1 = a_2$, $b_1 = b_2 = 0$.
(b) $\rho_1 = \rho_2 = 0$, when $\beta_1 + \beta_2 = 2\pi$, and equation (A 1) is satisfied.
(c) $\rho_1 = \rho_2 = \pm\pi$, when $\beta_1 = \beta_2$, and equation (A 2) is satisfied.

Considering $\{\boldsymbol{\rho}\}_v^2$, for a degree-2 single-vertex creased paper in case (a), the vertex and two inner creases can be merged into one inner crease; for case (b) or (c), this single creased paper can be regarded as a panel. For a degree-2 single-hole creased paper, case (a) can be regarded as two panels rotating along an inner crease. For case (b) or (c), the configuration space is trivial, which means they can be regarded as a panel. Therefore in a large creased paper we only need to consider at least degree-3 single creased papers.

For $n \geq 3$, it seems hard to make direct symbolic calculations and study the real roots. A possible way is to solve the polynomial system numerically, but the complexity increases rapidly. We then provide the result for $\{\boldsymbol{\rho}\}_v^3$ from the analysis on a spherical triangle, which is:

(a) i, j, k is a permutation of $\{1, 2, 3\}$. If

(a) $\alpha_i = \pi$, then $\alpha_j + \alpha_k = \pi$, $\rho_k = \rho_i$, $\rho_j = 0$.
(b) $\alpha_i + \alpha_j = \pi$, then $\alpha_k = \pi$, $\rho_k = \rho_j$, $\rho_i = 0$.

(b) If $\alpha_1 + \alpha_2 + \alpha_3 = 2\pi$ and not (a), $\rho_1 = \rho_2 = \rho_3 = 0$.
(c) Otherwise, there are two solutions $\{\rho_1, \rho_2, \rho_3\}$ and $\{-\rho_1, -\rho_2, -\rho_3\}$, which satisfy the following equations and the supplement of ρ_1, ρ_2, ρ_3 are the interior angles of a spherical triangle. (Special cases like $\alpha_i = \alpha_j + \alpha_k$ are included)

$$\begin{aligned} \cos\rho_1 &= \frac{\cos\alpha_1 \cos\alpha_2 - \cos\alpha_3}{\sin\alpha_1 \sin\alpha_2} \\ \cos\rho_2 &= \frac{\cos\alpha_2 \cos\alpha_3 - \cos\alpha_1}{\sin\alpha_2 \sin\alpha_3} \\ \cos\rho_3 &= \frac{\cos\alpha_3 \cos\alpha_1 - \cos\alpha_2}{\sin\alpha_3 \sin\alpha_1} \end{aligned} \tag{A 3}$$

As for a degree-3 single-hole creased paper, $\{\boldsymbol{\rho}\}_h^3$ is a subset of $\{\boldsymbol{\rho}\}_v^3$ and is not empty. Since it is not possible for a degree-3 single creased paper to have continous rigid folding motion different from folding along a single crease, we usually consider no less than degree-4 single creased papers.

Data Accessibility. This article has no additional data.

Authors' Contributions. ZH developed the fundamental framework described here, and took the primary role in writing the paper. SDG provided advice on the development of the project, made contributions to the theoretical framework and helped to write the paper. All authors gave final approval for publication.

Competing Interests. We have no competing interests.

Funding. We have no funding to declare for this article.

Acknowledgements. We thank Allan McRobie, Tomohiro Tachi, Robert Connelly, Thomas C. Hull, Walter Whiteley and Hellmuth Stachel for helpful discussions.

References

1. Callens SJ, Zadpoor AA. 2017 From flat sheets to curved geometries: Origami and kirigami approaches. *Materials Today*. doi: 10.1016/j.mattod.2017.10.004.
2. Debnath S, Fei LJ. 2013 Origami theory and its applications: A literature review. *World Academy of Science, Engineering and Technology* pp. 1131–1135.
3. Demaine ED, O'Rourke J. 2007 *Geometric folding algorithms*. Cambridge university press Cambridge. doi: 10.1017/CBO9780511735172.
4. Zorich VA. 2004 *Mathematical analysis* vol. 65. Springer. doi: 10.1007/978-3-662-48993-2.
5. Tachi T. 2010 Freeform variations of origami. *J. Geom. Graph* **14**, 203–215.
6. Demaine ED, Demaine ML, Hart V, Price GN, Tachi T. 2011 (Non) existence of pleated folds: how paper folds between creases. *Graphs and Combinatorics* **27**, 377–397. doi: 10.1007/s00373-011-1025-2.
7. Hull TC. 2002 Modelling the folding of paper into three dimensions using affine transformations. *Linear Algebra and its Applications* **348**, 273–282. doi: 10.1016/s0024-3795(01)00608-5.
8. Tachi T. 2015 Rigid folding of periodic origami tessellations. *Origami* **6**, 97–108. doi: 10.1090/mbk/095.1/10.
9. Tachi T. 2012 Design of infinitesimally and finitely flexible origami based on reciprocal figures. *Journal of Geometry and Graphics* **16**, 223–234.
10. Milnor J. 1968 *Singular Points of Complex Hypersurfaces*. Princeton University Press. doi: 10.1515/9781400881819-004.
11. Tachi T. 2009 Generalization of rigid-foldable quadrilateral-mesh origami. *Journal of the International Association for Shell and Spatial Structures* **50**, 173–179.
12. Tachi T. 2010 Geometric considerations for the design of rigid origami structures. In *Proceedings of the International Association for Shell and Spatial Structures (IASS) Symposium* vol. 12 pp. 458–460.
13. Spivak MD. 1999 *A comprehensive introduction to differential geometry*. Publish or perish.
14. Tay TS, Whiteley W. 1987 Chapter 7: Generic Rigidity (draft). http://wiki.math.yorku.ca/images/0/0f/Chapter7.pdf.
15. Bochnak J, Coste M, Roy MF. 2013 *Real algebraic geometry* vol. 36. Springer Science & Business Media.
16. Fowler PW, Guest SD. 2002 Symmetry analysis of the double banana and related indeterminate structures. In *New approaches to structural mechanics, shells and biological structures* pp. 91–100. Springer.
17. Miura K. 1985 Method of packaging and deployment of large membranes in space. *Title The Institute of Space and Astronautical Science Report* **618**, 1.
18. Katoh N, Tanigawa Si. 2011 A Proof of the Molecular Conjecture. *Discrete & Computational Geometry* **45**, 647–700. doi: 10.1007/s00454-011-9348-6.
19. Chen Y, Sareh P, Yan J, Fallah AS, Feng J. 2019 An Integrated Geometric-Graph-Theoretic Approach to Representing Origami Structures and Their Corresponding Truss Frameworks. *Journal of Mechanical Design* **141**, 091402. doi: 10.1115/1.4042791.
20. Schenk M, Guest SD. 2011 Origami folding: A structural engineering approach. In *Origami 5: Fifth International Meeting of Origami Science, Mathematics, and Education* pp. 291–304. CRC Press, Boca Raton, FL. doi: 10.1201/b10971-27.
21. Demaine ED, Demaine ML, Huffman DA, Hull TC, Koschitz D, Tachi T. 2016 Zero-Area Reciprocal Diagram of Origami. In *Proceedings of IASS Annual Symposia* vol. 2016 pp. 1–10. International Association for Shell and Spatial Structures (IASS).

22. Schief WK, Bobenko AI, Hoffmann T. 2008 On the Integrability of Infinitesimal and Finite Deformations of Polyhedral Surfaces. *Discrete differential geometry* pp. 67–93. doi: 10.1007/978-3-7643-8621-4_4.
23. Connelly R. 1977 A counterexample to the rigidity conjecture for polyhedra. *Publications MathÃl'matiques de l'IHÃL'S* **47**, 333–338. doi: 10.1007/bf02684342.
24. Connelly R, Sabitov I, Walz A. 1997 The bellows conjecture. *Beitr. Algebra Geom* **38**, 1–10. doi: 10.1038/scientificamerican0798-110.
25. Connelly R, Demaine ED, Rote G. 2003 Straightening Polygonal Arcs and Convexifying Polygonal Cycles. *Discrete & Computational Geometry* **30**, 205–239. doi: 10.1007/s00454-003-0006-7.
26. Streinu I, Whiteley W. 2004 Single-vertex origami and spherical expansive motions. In *Japanese Conference on Discrete and Computational Geometry* pp. 161–173. Springer. doi: 10.1007/11589440_17.
27. Abel Z, Cantarella J, Demaine ED, Eppstein D, Hull TC, Ku JS, Lang RJ, Tachi T. 2016 Rigid origami vertices: Conditions and forcing sets. *Journal of Computational Geometry* **7**, 171–184. doi: 10.20382/jocg.v7i1a9.
28. Wei G, Dai JS. 2014 Origami-Inspired Integrated Planar-Spherical Overconstrained Mechanisms. *Journal of Mechanical Design* **136**. doi: 10.1115/1.4025821.
29. Tachi T. 2009 Simulation of rigid origami. *Origami* **4**, 175–187. doi: 10.1201/b10653-20.
30. O'Rourke J. 2008 *Unfolding polyhedra*. Citeseer.
31. Bohlin R, Kavraki LE. 2000 Path planning using lazy PRM. In *Robotics and Automation, 2000. Proceedings. ICRA'00. IEEE International Conference on* vol. 1 pp. 521–528. IEEE. doi: 10.1109/robot.2000.844107.
32. Xi Z, Lien JM. 2015 Continuous unfolding of polyhedra-a motion planning approach. In *2015 IEEE/RSJ International Conference on Intelligent Robots and Systems (IROS)* pp. 3249–3254. IEEE. doi: 10.1109/iros.2015.7353828.
33. Hao Y, Kim Yh, Lien JM. 2018 Synthesis of fast and collision-free folding of polyhedral nets. In *Proceedings of the 2nd ACM Symposium on Computational Fabrication - SCF '18* pp. 1–10 Cambridge, Massachusetts. ACM Press. doi: 10.1145/3213512.3213517.
34. Aloupis G, Demaine ED, Langerman S, Morin P, O'Rourke J, Streinu I, Toussaint G. 2008 Edge-unfolding nested polyhedral bands. *Computational Geometry-Theory and Application* **39**, 30–42. doi: 10.1016/j.comgeo.2007.05.009.
35. Demaine ED, Demaine ML, Hart V, Iacono J, Langerman S, OâĂŹRourke J. 2011 Continuous Blooming of Convex Polyhedra. *Graphs and Combinatorics* **27**, 363–376. doi: 10.1007/s00373-011-1024-3.
36. Bern M, Hayes B. 1996 The complexity of flat origami. In *SODA* vol. 96 pp. 175–183.
37. Akitaya H, Demaine ED, Horiyama T, Hull TC, Ku JS, Tachi T. 2018 Rigid Foldability is NP-Hard. *arXiv:1812.01160 [cs, math]*. arXiv: 1812.01160.
38. Hull T, Chang E. 2011 Flat vertex fold sequences. In *Origami5: Fifth Int. Meeting of Origami Science, Mathematics, and Education* pp. 599–607. doi: 10.1201/b10971-51.
39. Ballinger B, Damian M, Eppstein D, Flatland R, Ginepro J, Hull T. 2015 Minimum forcing sets for Miura folding patterns. In *Proceedings of the Twenty-Sixth Annual ACM-SIAM Symposium on Discrete Algorithms* pp. 136–147. Society for Industrial and Applied Mathematics. doi: 10.1137/1.9781611973730.11.
40. Ginepro J, Hull TC. 2014 Counting Miura-ori foldings. *Journal of Integer Sequences* **17**, 3.